arXiv:2211.16733v2 [physics.soc-ph] 13 May 2023

Minor extensions of the logistic equation for growth curves of word counts on online media: Parametric observation of diversity of growth in society

Hayafumi Watanabe[1,2,3*]
Department of Economics, Seijo University, Setagaya-ku, Tokyo 157-8519, Japan
College of science and technology, Kanazawa University, Kanazawa-shi, Ishikawa 920-1192, Japan and
The Institute of Statistical Mathematics, Tachikawa-shi, Tokyo 106-8569,Japan

To understand the growth phenomena in collective human systems, we analyzed monthly word count time series of new vocabularies extracted from approximately 1 billion Japanese blog articles from 2007 to 2019. In particular, we first introduced the extended logistic equation by adding one parameter to the original equation and showed that the model can consistently reproduce various patterns of actual growth curves, such as the logistic function, linear growth, and finite-time divergence. Second, by analyzing the model parameters, we found that the typical growth pattern is not only a logistic function, which often appears in various complex systems, but also a non-trivial growth curve that starts with an exponential function and asymptotically approaches a power function without a steady state. We also observed a connection between the functional form of growth and the peak-out behavior. Finally, we showed that the proposed model and statistical properties are also valid for Google Trends data (English, French, Spanish, and Japanese), which is a time series of the nationwide popularity of search queries.

1. INTRODUCTION

For over 200 years, growth phenomena in complex systems such as human populations, biological populations, innovation, and language change have been studied quantitatively in social sciences, biology, and physics. The most basic description of the growth phenomena is the logistic equation proposed in 1838 by Belgian mathematician Pierre-François Verhulst to explain the population growth of some countries [1, 2],

$$\frac{dy(t)}{dt} = ry(t)\left(1 - \frac{y(t)}{Y}\right). \tag{1}$$

Here, $Y > 0$ is the carrying capacity (i.e., the maximum population that the environment can sustain indefinitely), and $r > 0$ is the growth rate. This equation is based on the exponential population growth effect and density effects (i.e., the effects of the population growth rate being suppressed by resource or environmental limitations). The solution to the logistic equation is the well-known logistic curve, which is also called the S-shaped curve, S-shaped curve, or S-curve.

$$y(t) = \frac{Y}{1 + (\frac{Y}{y(0)} - 1)\exp(-rt)}. \tag{2}$$

This discovery was forgotten until 1920, when Raymond Pearl and Lowell J. Reed rediscovered the logistic equation of the human population and showed experimentally that the equation could be adapted to the growth of the Drosophila population [2, 3]. For more than a century since this discovery, many researchers have applied the logistic equation or its extensions, such as bacterial populations and harbor seal populations (biological systems) [4, 5], language change and lexical diffusion (linguistic systems) [6, 7], diffusion of innovations, durable consumer goods, and growth of population and epidemic diseases (social and economic systems) [8–11]. Furthermore, extensions of the logistic equation have helped improve our understanding of the mathematics of nonlinear dynamics and complex systems, such as nonlinear oscillation and chaos [12].

In this study, to understand growth phenomena of large collective human systems, we systematically observe the growth phenomena in online languages and describe them with the least possible extension of the logistic equation, similar to previous studies. In addition, by using our introduced model with small parameters, we aim to clarify the typical macro growth dynamics and their diversity. This study provides systematically organized observations of collective human growth phenomena, which is a typical complex system; and the extension of the logistic equation allows us to associate online language growth phenomena with growth phenomena in previously studied complex systems.

Traditionally, growth phenomena in languages have been studied for many years in quantitative linguistics, historical linguistics and sociolinguistics. They have been studied in the context of "language change" and "lexical diffusion". Many studies have shown that a typical growth pattern is an S-curve (slow start, accelerating period, and slow end), and the sociolinguistic mechanisms behind the emergence of the S-curve have also been discussed [7, 13]. A quantitative fit of the S-curve to the logistic equation is known as Piotrovski's law, which was first reported by Piotrovskaja and Piotrovskij (1974) [14] and by Altmann et al. (1983) [15]. Subsequently, many studies have found various examples of the logistic-like S-curve, almost establishing that S-curves are the majority of language change in long-term time-scale (historical time-scale) [6]. For example, the replacement

*E-mail: hayafumi.watanabe@gmail.com

of "wszytec" with "wszystec (all)" in Polish from the 15th to the 18th century has an S-curve that can be well approximated by a logistic function (when plotted with time on the x-axis and the ratio of the replacement from "wszytec" to "wszytec" on the y-axis) [16]. Recently, with the increase in data, more precise verifications of the logistic equation or its extension models have been examined [13, 16–19].

The main features of our study compared to these traditional studies are (i) the time scale (the time scale of traditional studies is a historical scale or more than 100 years with a time resolution of years, whereas that of our study is 5 or 10 years and its time resolution of months) and (ii) the diversity of vocabulary (e.g., the word set of our study includes the recent online language, and we aim to describe the diversity of growth curves as simply as possible). An example of a previous study on word count growth in online social media, which satisfies the above two conditions, is Ref. [19]. The author examined the S-curve for several words on Twitter, which is a well-known social media or microblogging service, and claimed that there are both S-curve and non-S-curve type growth curves depending on the words. Our study can also be regarded as a more precise version of this previous study.

From a practical standpoint, the time series of word counts in nationwide social media is used to quantify temporal changes in social interests [20] and is also used as a marketing tool to observe diffusion of new things such as new ideas, technologies, and new products. Diffusion (growth) phenomena such as ideas, products, and innovations have traditionally been studied for more than a century in sociology and business science as "innovation diffusion" or "product diffusion". Many studies have discussed the relationship between diffusion and logistic-like S-curves. Pioneering work on logistic-like S-curve growth phenomena is the growth of new types of social institutions by SF. Stuart Chapin in 1928 [21], agricultural technology by Bryce Ryan and Neal C. Gross et al. in 1943 [22], and one of the most famous and representative work is "Diffusion of Innovations" by Everett M. Rogers in 1962 [8]. Influenced by Roger's work, an extension of the logistic equation, the Bass model, developed by Frank Bass in 1969, is still often used to describe the process of how new products are adopted by a population.

$$\frac{dy(t)}{dt} = (ry(t) + \alpha)\left(1 - \frac{y(t)}{Y}\right), \tag{3}$$

where $\alpha \geq 0$ and $Y > 0$ are constants [9, 10, 23]. Our study also corresponds to quantitative measurements of the diffusion of new products and ideas using linguistic data. Hence, the proposed model and its findings may contribute to innovation diffusion research as a tool for quantitative observation.

Note that physicists have studied linguistic phenomena using the concepts of complex systems [24], such as competitive dynamics [25], statistical laws [26–28], and complex networks [29]. Our research can also be regarded as the study of language phenomena from the perspective of physics or complex systems. In particular, restricting the field to the study of dynamics of words counts daily or monthly time series, the noise structure [30] and dynamics of a "mature phase" in the life trajectory of words [31, 32], consisting of an "infant phase", an "adolescent phase" (i.e., the phase of growth in society) and a "mature phase" (i.e., the phase of well-established in society), are previously shown. In contrast, this study focuses on the infant and adolescent phases. It is notable that in Ref. [28], authors discussed the relationship between vocabulary growth and linguistic statistics on historical time scales by using the word frequencies data in printed books from 1520 to 2000 from physics or complex systems perspective. Also in Ref. [33], the author clearly observed the linear preferential attachment (i.e. the rich-get-richer phenomenon) in word-count time series on the same data, and showed its relation to Zipf's law. Furthermore, the same author showed that this relationship between preferential attachment and Zipf's law is also valid for words used in physics papers in the last 100 years [34]. The preferential attachment effect presented in Ref. [34], where the speed of growth is proportional to the word frequency, is one of essential elements of the logistic equation given by Eq. 1.

In this study, we first briefly describe the two types of word count time-series data used in our study: Japanese blog data and the Google Trends data. Second, we introduce an extension of the logistic equation in Eq.4 to describe the time series data. Third, by analyzing the data, we show that the model can consistently reproduce various patterns of actual growth curves, such as the logistic function, linear growth, and finite-time divergence. Fourth, by analyzing the model parameters of the actual data, we investigate the typical patterns and diversity of growth dynamics and the forecasting ability of the proposed model. Fifth, we confirm that the proposed model and its properties are adaptable to Google search data in English, French, Spanish, and Japanese. Finally, we provide our conclusions and discussions.

2. DATA

We employed two types of online language data: (a) Japanese blog data, and (b) Google Trends (English, French, Spanish, and Japanese). From this data, we extracted the word-count time series for analysis.

2.1. Japanese blog data

We obtained the time-series of word appearances per day in nationwide Japanese blogs using a large database of Japanese blogs ("Kuchikomi@kakaricho"), which was provided by Hottolink, Inc. This database contains nine billion articles on Japanese blogs, which covers 90 percent

of Japanese blogs from November 1, 2006, to December 31, 2019 [35–37].

a. Word selection We extracted 20,764 new words from one million Wikipedia title words during the observation period. Specifically, we used the following procedure. First, we extracted the top one million high-frequency words from the list of titles of articles in the Japanese version of Wikipedia [38]. Here, the frequency is measured by the blog dataset, namely, the total number of blog posts with a focused title word during the observation period. Second, we extracted 20,764 newly appearing words from the 1 million candidate words, which were defined as words that did not appear in blogs before 2016 (i.e., words with a total frequency of 0 in 2016). The details of word selection are provided in Appendix A3.

b. Normalized time series of word appearances We define the notation of the time series of word appearances $x_j(t)$ and $y_j(t)$ as follows:

- We set the time step at 30 days. When the time stamp advances by one, real time advances by 30 days (almost a monthly time series).
- $x_j(t)$ $(t = 1, 2, \cdots T)$ $(j = 1, 2, 3, W)$ is the raw count of the articles containing the j-th word for 30 days at the time t within the dataset.
- $y_j(t) = x_j(t)/m(t)$ is time-series of the count of the articles containing the j-th word normalized by the (scaled) total number of articles $m(t)$ (see the black triangles in Fig. 1 and Fig. 2).

where T is the last observation time, W is the number of words, $m(t) = M(t)/(\sum_{t=1}^{T} \frac{M(t)}{T})$ is the scaled total number of articles, and $M(t)$ is the time series of the total number of articles over 30 days. Note that $y_j(t)$ corresponds to the original time deviation of the j-th word separated from the effects of deviations in the total number of articles $M(t)$ (see Fig. 1 in Ref. [30]).

2.2. Google Trends

Google Trends is a monthly time series of the number of searches for a focused word using the Google search engine provided by Google Inc. [20]. Similar to the number of blog posts, it is used to quantify social interests (see the red crosses in Fig. 2). Google Trends was normalized to 100 for the maximum value of the observation period. The data is available since May of 2015.

We selected new words from the lists of titles of articles in the English, French, Spanish or Japanese versions of Wikipedia [38]. Specifically, we used the following procedure: we selected the titles of articles whose annual Wikipedia page views were 0 on May 1, 2015, and more than 50 page views (for French, Spanish and Japanese) or 1000 page views (for English) on January 1 of 2016, 2017,$\cdots$, 2021 or 2022 [39]. The details of word selection are provided in Appendix A3.

3. EXTENSION OF THE LOGISTIC EQUATION

To describe the growth of word counts in online media, we extend the logistic equation by adding a power-law exponent α as follows:

$$\frac{dy(t)}{dt} = ry(t)\left(1 + \frac{y(t)}{Y}\right)^{\alpha} \tag{4}$$

where $y(t) > 0$ is the word count at time t and $Y \neq 0$ is the transition point. For the logistic equation ($\alpha = 1, Y < 0$), Y is the carrying capacity (i.e., the maximum sustainable population). $r > 0$ is the growth rate for $y(t) \ll Y$; that is, the case of the population $y(t)$ is very small compared to the transition point Y. The model for $Y < 0$ corresponds to the special case of Blumberg's equation or generalized logistic equation [10]. In this paper, we call this model as the proposed model.

From Appendix A2, the time evolution of the equation can be qualitatively classified into four categories based on the signs of parameters Y and α:

1. Convergence to a constant (S-curve) ($Y < 0$, $\alpha > 0$).
2. Finite-time divergence (Deadline effects) ($Y > 0$, $\alpha > 0$)
3. Divergence after infinite time (Asymptotic power-law function) ($Y > 0$, $\alpha < 0$)
4. Finite-time divergence of first-order derivatives ($Y < 0$, $\alpha < 0$).

Examples of words in each category are given in Appendix A8.

For the parameters $\alpha > 0$ and $Y < 0$, which correspond to the first case, the equation corresponds to the S-curve. For $\alpha = 1$, the word count $y(t)$ increases the logistic function (symmetric S-curve) given by Eq. 2 and for $\alpha \neq 1$, $y(t)$ growth the asymmetric S-curve (Fig. 1 (j)).

For the parameter $\alpha > 0$ and $Y > 0$, which corresponds to the second case, $y(t)$ obeys the finite-time divergence known as the deadline effect. The deadline effect is a phenomenon in which interest increases with a power function toward a deadline t^* [40],

$$y(t) \propto \frac{1}{(t^* - t)^{\beta}}, \tag{5}$$

where $\beta > 0$ is the power-law exponent. For instance, when $\alpha = 1$, $y(t) \gg Y > 0$, using the approximation of Eq. 4,

$$\frac{dy(t)}{dt} \sim ry(t)\left(\frac{y(t)}{Y}\right)^{1}, \tag{6}$$

we can easily obtain the deadline-effects solution

$$y(t) \propto \frac{Y}{Y/(y(0) \cdot r) - t}. \tag{7}$$

This effect has been observed in various phenomena with scheduled deadlines, such as an application for an international conference [40] and numbers of blog posts for annual events like Christmas, Olympic Games and a launch of a new product that has been announced in advance (Figs. 1 (g),(h),(i) and Figs. 2 (b), (c)).

The parameter $\alpha < 0$, $Y > 0$, which corresponds to the third case, can express growth asymptotically slower than exponential growth. For example, in the case where $\alpha = -1, Y > 0$, for $y(t) \gg Y$, the approximation of Eq. 4,

$$\frac{dy(t)}{dt} \sim ry(t)\left(\frac{y(t)}{Y}\right)^{-1} = rY \tag{8}$$

we can also obtain a linear solution

$$y(t) \sim rYt + y(0) \propto t. \tag{9}$$

This linear behavior was also confirmed in our data concerning the growth of word counts for the names of local boroughs or administrative facilities (see Fig. 1(b)).

The exact solution of the equation given by Eq. 4 can be solved as a variable separation form,

$$t = t_0 + \frac{1}{r}\int_{1+y(t_0)/Y}^{1+y(t)/Y} \frac{1}{(1-x)\cdot x^{\alpha}} dx \tag{10}$$

$$= t_0 + \frac{1}{r}(B_\alpha(1+y(t)/Y) - B_\alpha(1+y(t_0)/Y)) \tag{11}$$

By introducing the inverse function, we can formally write the solution as

$$y(t) = Y\left(B_\alpha^{-1}(r(t-t_0) + B_\alpha(1+y(t_0)/Y)) - 1\right), \tag{12}$$

where

$$B_a(v) \equiv \begin{cases} (a=1) \\ \frac{1-v}{|1-v|}\log(|1-v|) + \log(v) \\ (a = 2, 3, \cdots) \\ \frac{1-v}{|1-v|}\log(|1-v|) + \log(v) + \sum_{i=2}^{a} \frac{1}{-i+1} v^{-i+1} \\ (others) \\ \frac{v^{1-a}\,{}_2F_1(a, 1-a; 2-a; v)}{1-a} \end{cases}$$

${}_2F_1(a, b; c; x)$ is the Gauss hypergeometric function and the inverse function of $B_\alpha(x)$ is denoted by $B_\alpha^{-1}(t)$. Here, $B_\alpha^{-1}(B_\alpha(x)) = x$, $0 < B_\alpha^{-1}(t) < 1$ for $Y < 0$ and $B_\alpha^{-1}(t) > 1$ for $Y > 0$. Details of the derivation of the solution are given in Appendix A1.

4. VALIDATION OF THE MODEL WITH ACTUAL DATA

We validated the proposed equation in three ways using real data. Note that in this section, we analyze only the growth domain, which was extracted using the method described in Appendix A4. Examples of the growth domains are the domains between the gray vertical dashed lines in Fig. 2. Furthermore, words with a growth period of less than 12 points (approximately one year) were excluded from our analysis.

In the Appendix A7, we examine the proposed model in more detail. For example, we compare the proposed model with models not discussed in this section.

4.1. Example of verification by individual time series

Figs. 1 show typical time series of word counts in the blog data. We can confirm that the curves given by Eq. 4 (the red dashed lines) are well in agreement with the most of the actual time series (black triangles), the proposed model Eq. 4 can comprehensively describes various patterns of growth of the word time series. For example, the linear growth for $\alpha \sim -1, Y > 0$ is shown in panel (b), the finite-time divergence $\alpha \sim 1, Y > 0$ in panel (h), and the S-curve $\alpha \sim 1, Y < 0$ in panel (j). The tuning parameters of the model, α, Y, r, were estimated by minimizing the mean absolute error with regularization. The details of the parameter tuning are shown in Appendix A5.

4.2. Statistical verification of the shapes of a growth curve

Second, we demonstrate that Eq. 4 holds not only for individual time series, but also for the statistics of the entire dataset. By transforming the time series $y_j(t)$ and obeying the dynamics in Eq. 4, we can derive the word-independent relationship,

$$z_j(t) = t_0 + \frac{1}{r}(B_\alpha(1+y_j(t)/Y) - B_\alpha(1+y_j(t_0)/Y)) = t, \tag{13}$$

where we use Eq. 11. Taking the ensemble median for words in this transformed time series $z_j(t)$, we can also obtain the simple relation,

$$\hat{z}(t) = Median_j[z_j(y_j(t))] = t. \tag{14}$$

This statistical relationship was used to validate the data.

The black triangles (which appear as a black line) in Fig. 3(a) indicates $\hat{z}(t)$ given by Eq. 14 of the real data. The straight line illustrated by triangles implies that $\hat{z}(t)$ for the actual data reproduces Eq. 11, mainly, the time series of word counts are consistent with the dynamics of the proposed model given by Eq. 4 statistically. Note that the 10th and 90th percentiles shown in grey dashed lines are also almost straight lines, in the same way as the 50th percentile given by Eq. 14.

We also check that Eq. 14 (i.e., dynamics given by Eq. 4) holds on actual data independently of the parameters α and Y. We introduced an ensemble median conditioned

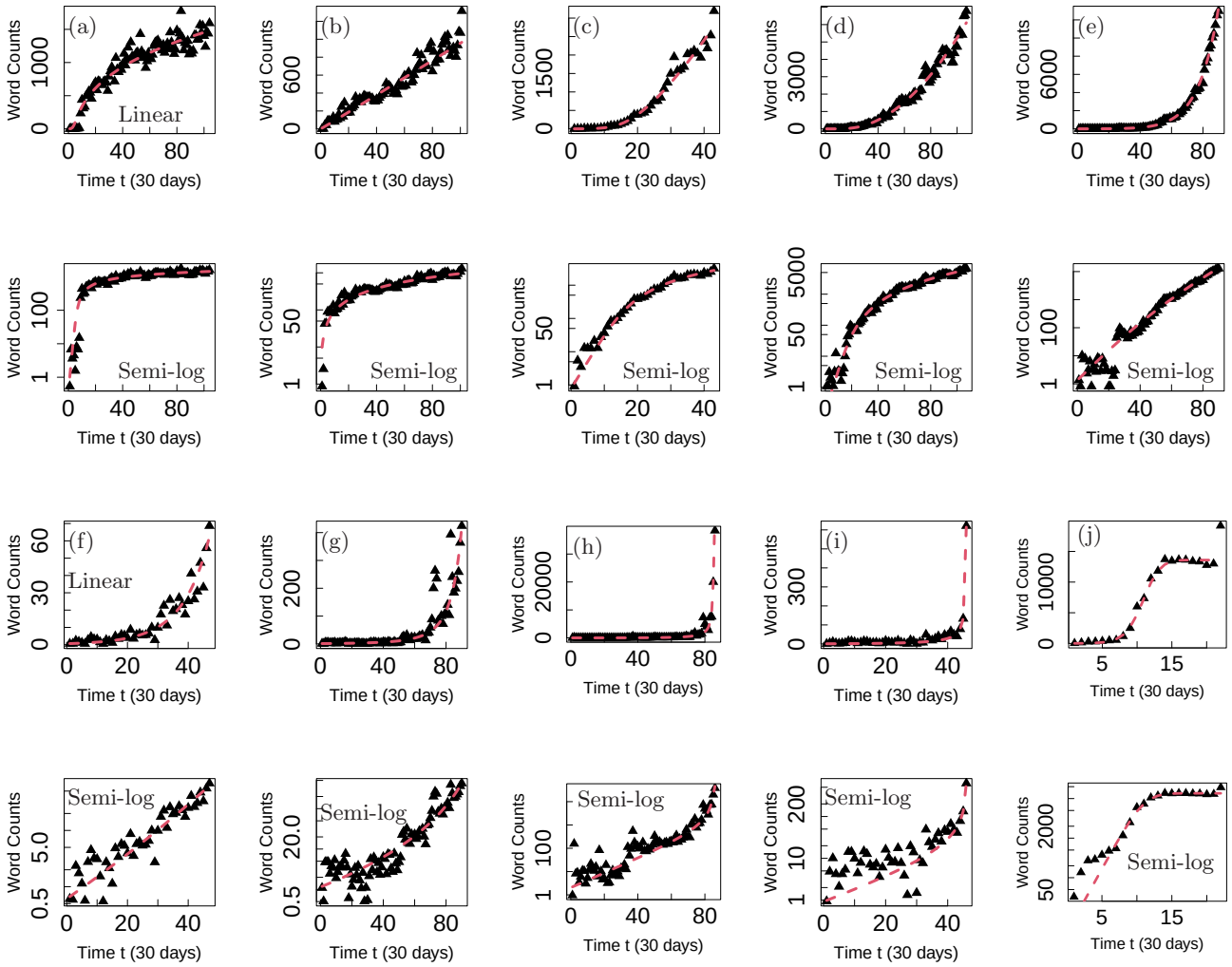


FIG. 1: Examples of time series of the growth process of word counts in Japanese blogs. The black triangles are the real data $y_j(t)$ and the red dashed line is the corresponding theoretical line. Parameters were determined by Appendix A5. The upper figure is a linear plot, and the lower figure is the corresponding semilog plot. (a) Pinterest (Web service) $\alpha = -3.07, Y = 262.5, r = 1.41, y(0) = 0.374$ (b) SagamiharaShiTyuuouKu (Sagamihara city central ward, new place name) $\alpha = -0.994, Y = 1.14, r = 8.13, y(0) = 2.13$ (c) Komyusyou (People who are not good at social interactions and get nervous, Internet slang) $\alpha = -0.799, Y = 221, r = 0.376, y(0) = 0.775$ (d) KuraudoFandingu (Crowd funding, Business or Internet Term) $\alpha = -0.512, Y = 31.0, r = 0.317, y(0) = 0.159$ (e) OnlineSaron (Online salon, which is an online community service with a fixed fee, hosted by celebrities or well-known executives etc.) $\alpha = -0.0742, Y = 31.4, r = 0.121, y(0) = 1.35$ (f) Puurui (Pour Lui, Name of a new Japanese singer) $\alpha = 0.0884, Y = 2.49, r = 0.0872, y(0) = 0.610$ (g) JyoseiKatuyakuSuisin (Promotion of Women's Participation and Advancement in the Workplace, Name of Japanese Government Policy) $\alpha = 0.262, Y = 0.690, r = 0.0282, y(0) = 1.15$ (h) RioGorin (Rio de Janeiro Olympics, Sports events) $\alpha = 0.859, Y = 806, r = 0.0725, y(0) = 2.05$ (i) DesumaatikaraHajimaruIsekaiKyousoukyoku (Death March to the Parallel World Rhapsody, Titles of Japanese novels for young people) $\alpha = 2.27, Y = 90.4, r = 0.0748, y(0) = 0.922$ (j) Pazudora (Puzzle and Dragons, Name of a puzzle video game) $\alpha = 0.88, Y = -13593, r = 0.741, y(0) = 4.12$

on α and the sign of Y denoted by s_Y taking 1 or -1 as follows:

$$\hat{z}(t|\alpha, s_Y) = Median_{\{j|\alpha-d\leq\alpha_j<\alpha+d, sign(Y_j)=s_Y\}}[\hat{t}_j(z_j(t))] = t, \quad (15)$$

where $d = 0.5$ for $Y > 0$ or $d = \infty$ for $Y < 0$ is the box size for obtaining the statistics, and $Median_{\{S\}}[x]$ is the median x over the set S. The fact shown in Fig. 3(a) that the lines with different colors and shapes are overlapping enough to hide each other means that the word count data consistent with the dynamics Eq. 4, regardless of the main parameters α and Y, where green circles indicate $[\alpha = 0.5, Y > 0]$; green pluses $[\alpha = 1.0, Y > 0]$,

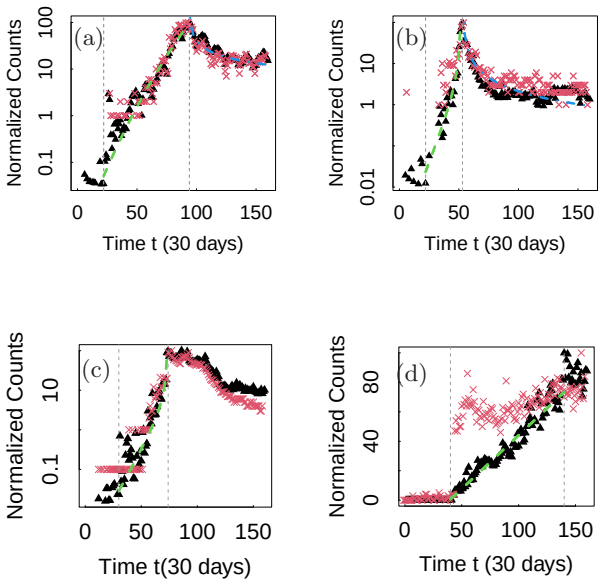


FIG. 2: Comparison of time series between blog data (black triangles) and Google Trends (red crosses). Blog data is scaled to a maximum value of 100. The green dashed line indicates the theoretical curve given by the model Eq. 4. and blue dashed line is power-law function $\propto \tau^{-0.5}$ in the panne (a) and $\propto \tau^{-1.0}$ in the panel(b). The area between the grey dotted lines is the growth period detected by adapting the method described in Appendix A4. (a) Asaii-Bouru (Açaí na tigela ,Brazilian dessert, $\alpha = -0.0722, Y = 1.14, r = 0.142, y(0) = 1.09$), (b) RabuTyuunyuu ("Love Injection", A silly joke phrase by an once-popular Japanese comedian, $\alpha = 0.661, Y = 158, r = 0.179, y(0) = 1.70$), (c) Windows8 (Windows 8, Famous software name, $\alpha = 1.041, Y = 276.2, r = 0.120, y(0) = 1.08$) and (d) SagamiharaShiTyuuooKu (Sagamihara city central ward, Place name, $\alpha = -0.994, Y = 1.15, r = 8.13, y(0) = 2.13$).

triangles up and down $[\alpha = 1.5, Y > 0]$; blue diamonds $[\alpha = -0.5, Y > 0]$,blue triangles pointing down for $[\alpha = -1, Y > 0]$, blue stars for $[\alpha = -1.5, Y > 0]$; purple crosses for $[Y < 0]$.

Finally, we confirmed that the simpler linear normalization and Bass model given by Eq. 3 cannot describe the actual data. The simple linear normalizations are shown in Fig. 3(c). From this figure, we confirm that linear normalization converts data with different parameters into a common curve. In the figure, the horizontal axis is standardized by the total growth period,

$$t'_j = t/T_j, \tag{16}$$

where T_j is the length of the growth period of j-th word.

The vertical axis is scaled by the median of the time series:

$$y'_j(t) = y_j(t)/Median_{\{t=1,2,\cdots,T_j\}}[y_j(t)], \tag{17}$$

and in the same manner as in Eq. 15, we plot the ensemble median conditioned on the parameters α and the sign of s_Y (i.e, $s_Y = sign(Y)$):

$$\hat{y'}(t'|\alpha, s_Y) = Median_{\{j|\alpha-\delta\leq\alpha_j<\alpha+\delta, sign(Y_j)=s_Y\}}[y'_j(z_j(t'_j))], \tag{18}$$

where in the case that $y'_j(t')$ is not observed data, we estimate it by linear interpolation from the data before and after observing $y'_j(t')$. This result implies the trivial fact that the shape of the growth curves depends on parameters α_j and Y_j.

The black triangles in Fig. 3(d) are the statistics of the time series transformed by the Bass model given by Eq. 3, corresponding to Fig. 3(a) for the proposed model given by Eq. 4. The fact that this plot is not the straight line $y = x$ shown in the red dashed line indicates that the Bass model cannot accurately describe the real data.

4.3. Verification by forecasting ability

The fit (i.e., training error) of the extended model given by Eq. 4 is always better than the logistic equation given by Eq. 1 theoretically because the extended model includes the logistic equation as the special parameter (i.e., $\alpha = 1$, $Y < 0$). Here, we compared the forecasting ability of the models to check for overfitting. If the forecasting ability of the extended model is lower than that of the logistic equation, the extension is meaningless, and the model can be considered overfitting. To check for overfitting, we estimated the model parameters using the first 70 percent of the time series from the beginning of the growth period and predicted the remaining 30 percent of the time series. The absolute mean error was used to measure the prediction accuracy:

$$\delta_j^{(model)} = Mean_{\{t|0.70T_j\leq t\leq T_j\}}[|\hat{y}_j(t) - y_j(t)|], \tag{19}$$

where $Mean_{\{t|t\in S\}}[x(t)]$ is the mean of the data for t that satisfies set S and $\hat{y}_j(t)$ is the predicted value of the jth word at time t from a model, such as the proposed model or the logistic equation.

Table I shows the winning ratio of the proposed model (i.e., the ratio of words for which the proposed model has a higher prediction accuracy than the comparison model). The winning ratio of the proposed model to the other models is defined as

$$R^{(model)} = \frac{\sum_{\{j|\delta_j^{(model)}>\delta_j^{(0)}, j\in W_s\}} 1}{\sum_{\{j|\delta_j^{(model)}>\delta_j^{(0)}, j\in W_s\}} 1 + \sum_{\{j|\delta_j^{(model)}<\delta_j^{(0)}, j\in W_s\}} 1}, \tag{20}$$

where W_s is the set of focused words with a sample size of 12 or more in the training data and $\delta_j^{(0)} = \delta_j^{(proposed)}$ is the absolute mean error of the proposed model given by Eq. 4. For $R^{(model)} > 0.5$, there are more words for which the proposed model has a smaller prediction error than the comparison model (roughly, the proposed

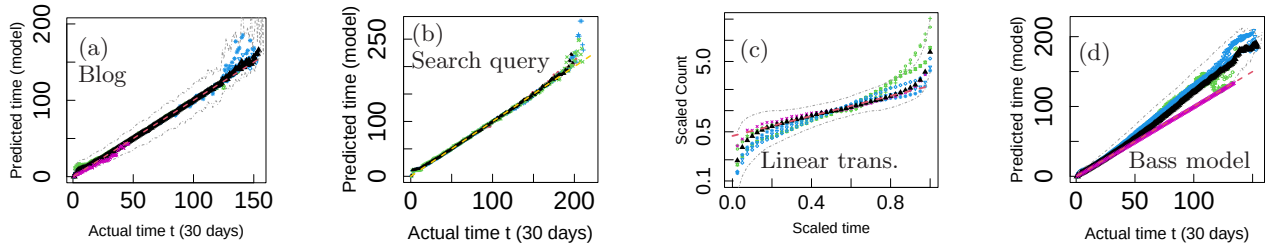


FIG. 3: Statistical verification of the proposed model given by Eq.4.
(a) Verification of blog data by using the statistical relation $\hat{z}(t|\alpha, s_Y) = t$ given by Eq. 15 (On calculating this relation, we predict t from y by using the proposed model given by Eq. 11). x-axis corresponds to actual time, y-axis corresponds to predicted time by the model and the red dashed line is $y = x$. In case of $Y > 0$ ($s_Y = sign(Y) = 1$), we plotted in green circles for $\alpha = 0.5$, pluses for $\alpha = 1.0$, for triangles up and down $\alpha = 1.5$ and blue diamonds for $\alpha = -0.5$, triangles point down for $\alpha = -1.0$ and in the case of $Y < 0$ ($s_Y = -1$), we plotted magenta crosses. We also plot the ensemble median over all data $\hat{z}(t)$ given by Eq. 14 in black triangles and the corresponding 10th and 90th percentiles are shown in gray dashed lines. The same straight line $y = x$, independent of α and Y means that the word counts are statistically consistent with the dynamics described by the proposed model given by Eq. 4.
(b) The corresponding figure of the panel (a) for Google Trends data and proposed model given by Eq .4. We plot the ensemble median over all the data $\hat{z}(t)$ given by Eq. 14. The yellow dashed line is $y = x$. The data are shown in black triangles for Japanese, red circles for French, green crosses for Spanish, and blue pluses for English.
(c) Ensemble median of time series scaled for time and word count by using the linear transformation $\hat{y}'(t'|\alpha, s_Y)$ given by Eq. 18. The ensemble was taken conditionally by parameters α and sign of Y, s_Y in the same way as the panel (a). From the panel, we can see that the x-axis and y-axis are both scaled, but the functional form is different for each α, s_Y.
(d) The corresponding figure of the panel (a) for the Bass model given by Eq. 3. From curves not obeying the straight line $y = x$, the word count data are conducted with the dynamics described by the bass model given by Eq. 3. Note that in panel (d), the parameters used for conditioning (color differences) are different from those used for prediction (i.e., Bass model). In the conditioning, we use the parameters of the proposed model and not the parameters of the Bass model.

model has a better prediction ability). Conversely, for $R^{(model)} < 0.5$, there are more words for which the proposed model has a larger prediction error than the comparison model (roughly, the proposed model has a lower prediction ability).

From Table I, we can confirm that the predictive ability of the proposed model is improved over that of the logistic equation in terms of the winning ratio ($R^{(logistic)} = 0.64$). We can also confirm that the Bass model, given by Eq. 3 also has less predictive ability than the proposed model ($R^{(Bass)} = 0.67$).

In addition to the logistic equation and Bass model, we compared its predictive ability with commonly used general time-series models, the SARIMA model (Seasonal Autoregressive Integrated Moving model) [41], which is one of the most well-known, traditional, and representative statistical time series models, and the Prophet model [42], which is a recently developed time-series model. These models, with a larger number of tuning parameters, can describe more complex structures than the proposed model. The forecasting ability in terms of the winning ratio is equivalent or higher than that of both the SARIMA model ($R^{(SARIMA)} = 0.52$) and Prophet model ($R^{(Prophet)} = 0.59$). Details and comparisons of predictive ability with other models are discussed in Appendix A7 and are shown in Table A1.

Logistic	Bass	SARIMA	Prophet
0.64 [0.63,0.65]	0.67 [0.66,0.68]	0.52 [0.51,0.53]	0.59 [0.58,0.60]

95% confidence intervals in brackets.

TABLE I: Winning ratio of prediction errors of the proposed model to other models

α/K	-1	+1
-1	11	8868
+1	1323	4303

TABLE II: Number of samples grouped by sign of α and Y

5. APPLICATIONS OF THE MODEL

In this section, we describe the application of the proposed model given by Eq. 4 to the analysis of growth phenomena in online social media.

5.1. Statistics of model parameters

First, we examined the statistics of the parameters of the proposed model given by Eq. 4. These statistics of

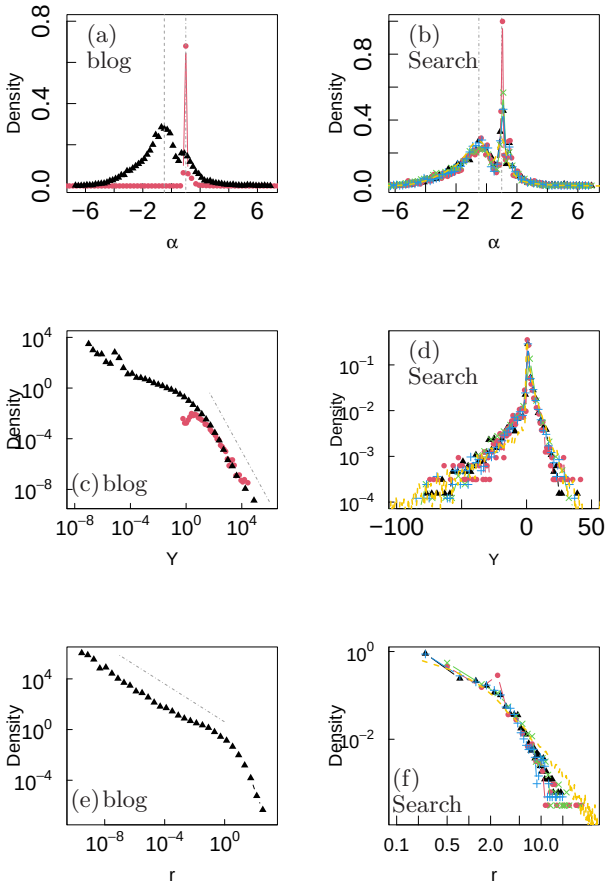


FIG. 4: Probability density function for α, Y, and r. (a) Distribution of α for blog data. Black triangle indicate the data for $Y > 0$, red circles for $Y < 0$. The vertical grey dashed lines are $\alpha = -0.5$ and $\alpha = 1$. From the figure, we can see that the most typical values are $\alpha \sim -0.5$ for $Y > 0$, and $\alpha \sim 1$ for $Y < 0$ (i.e., the logistic function). (b) Distribution of α for Google Trends data and blog data. The data is shown in black triangles for Japanese, blue pluses for English, red circles for French, green crosses for Spanish, and the yellow dashed line for the blog data. The vertical grey dashed lines are $\alpha = -0.5$ and $\alpha = 1$. The graph shows that all data have peaks at $\alpha \sim -0.5$ and $\alpha \sim 1$. (c) Distribution of $|Y|$ for blog data. We added the $\propto x^{-2}$ (the Zipf's law) shown in dotted lines. Black triangles indicate the data for $Y > 0$, red circles for $Y < 0$. (d) Distribution of Y for Google Trends data and blog data. The colors and shapes correspond to the panel (b). For the blog data, we plot $Y' = 100 \times Y/max(y(t))$ to match the Google Trends data maximum of 100 constraints. (e) Distribution of r for blog data. The colors and shapes correspond to the panel (a). We added the $\propto x^{-0.75}$ shown in dotted lines. (f) Distribution of r for Google Trends data and blog data. The colors and shapes correspond to the panel (b).

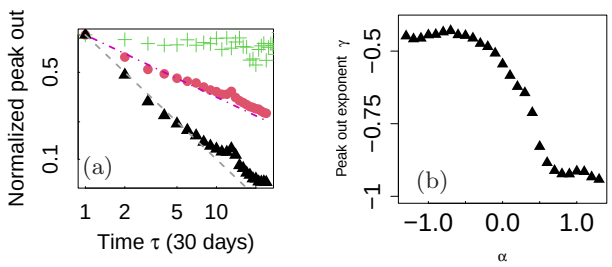


FIG. 5: (a) The behavor of peak-out in the log-log plot. Horizontal axis is time from peak. The vertical axis is the ensemble median of peak-out standardized to 1 at the peak $\hat{v}(\tau|\alpha, s_Y)$ given by Eq. 21. We plotted in black triangles conditioned by $\alpha > 0$, $Y > 0$, Red circles by $\alpha < 0$, $Y > 0$ and green pluses by $Y < 0$. We can see that the power-law decay depends on the sign of α and Y. (b) Relationship between α and the exponent γ for $Y > 0$, where the power-law decay is $\propto \tau^{\gamma}$. We can see the transition from $\gamma \sim -0.5$ to $\gamma \sim -1.0$.

parameters are expected to reflect the degree of diversity in dynamics.

Fig. 4 shows the probability density functions of α, Y and r. From panel(a), in the case that $Y > 0$, $\alpha \sim -0.5$ is the most frequent value (indicated by red circles), which corresponds asymptotically to power-law growth ($\propto t^2$). On the other hand, when $Y < 0$, $\alpha = 1$ is the most frequent (shown in black triangles), which corresponds to the logistic equation. Moreover, from panels(c) and (e), the distributions of Y and r have power-law-like heavy tails, respectively.

Second, we checked the correlations between the parameters. From Table II, we can confirm that there are relatively few words with both negative parameters $\alpha < 0$ and $Y < 0$. However, no other clear correlations were found.

5.2. Behavior after peak

The proposed model given by Eq. 4 does not tell us any information about the post peak-out behavior. In other words, the model describes only the growth period, such as the time period between the grey vertical lines in the time series in Fig 2. Thus, we empirically investigated the relationship between peak behavior and the behavior during growth (i.e., the parameters of the proposed model).

Fig. 5(a) shows the ensemble median of the peak-out behavior. Specifically, we calculate that the median of the normalized time series, which is normalized to the

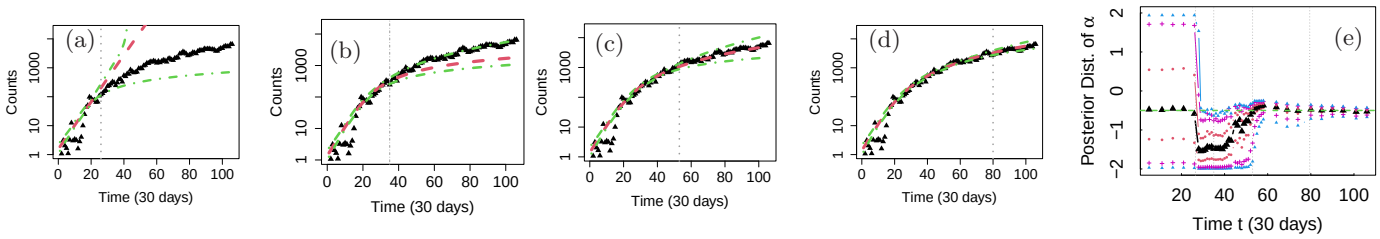


FIG. 6: Time series forecasting using the proposed model given by Eq. 4. (a)-(d) Comparison of time series of real data and time series predicted by the model. The black triangles are real data for "crowd funding" (the same word as Fig. 1 (d)). The prediction lines are the red dashed line for the median, the green dashed line for the 1st and 99th percentile points, where the prediction uses Bayesian modelling, as shown in Appendix A6, and the percentiles are calculated with their posterior distributions. We used the data to the left of the grey dotted line to make our prediction. The training data are $t \leq 26$ for the panel(a), $t \leq 37$ for the panel (b) $t \leq 53$ for the panel (c) and $t \leq 80$ for the panel (d). We can confirm that the prediction improves with more training data.
(e)Dependence of the posterior distribution of α on the training data. The graph shows the posterior distribution of α when using the training data to the time indicated by the x-axis. The data shown in black triangles is blue for 50 percentile, red circles for 25 percentile and 75 percentile, magenta pluses for 5 percentile and 95 percentile and blue triangles for 1 percentile and 99 percentile. The green horizontal dashed line is $y = 0.5$ and the grey vertical dashed line corresponds to the training data in (a)-(d). The posterior distribution of α converges from a prior distribution (the uniform distribution of -2 to 2) to $\alpha \sim -0.5$ as the training data increases.

peak at $t_j^{(max)}$ is 1,

$$\hat{v}(\tau|\alpha, s_Y) = Median_{\{j|\alpha-\delta_1\leq\alpha_j<\alpha+\delta_2, sign(Y_j)=s_Y\}}\left[\frac{y_j(\tau + t_j^{(max)} - 1)}{y_j(t_j^{(max)})}\right] \quad (21)$$

where τ is the time step from the peak, we take the median conditioned by the parameters α, s_Y taking 1 or -1 (i.e., the sign of Y) and $t_j^{(max)} = argmin_t\{y_j(t) \geq 0.999 \times y_j(T_j)\}$.

From Fig. 5(a), we can see that in the case of $Y < 0$, the peak out is a gradual decrease, as expected because the logistic-type equation asymptotically approaches Y for $t \to \infty$. On the other hand, in the case of $Y > 0$, the peak-out is a power-law decay whose power-law exponent depends on the parameter α. For $\alpha < 0$ (i.e., the infinite-time divergence case), the decay can be approximated as $\hat{v}(\tau) \propto \tau^{-0.5}$, and for $\alpha > 0$ (the finite-time divergence case), the decay can be approximated as $\hat{v}(\tau) \propto \tau^{-1}$.

The Fig. 5(b) shows the dependence of the exponent γ on α for $Y > 0$ when the peak out is approximated by a power function $\hat{v}(\tau|\alpha, s = 1) \propto \tau^{\gamma(\alpha)}$. In this figure, the data are grouped by α, and the power exponents are estimated as coefficients of linear regression in the log-log plots. From this figure, the exponent of the peak-out γ transitions from approximately -0.5 to approximately -1.0 depending on α.

Fig. 2 displays example of the time series of the peak out. Fig. 2(a) and Fig. 2(b) show the cases $\alpha = -0.0722$, $\gamma = -0.5$ and $\alpha = 0.661$, $\gamma = -1.0$, respectively. These results are not inconsistent with the overall statistics shown in Fig. 5. On the other hand, panels (c) and (d) show examples where the peak-out differs from the power decay. This figure implies that individual time series sometimes differ from the overall statistics.

Note that the power decay of exponent $\gamma = -0.5$ or $\propto \tau^{-0.5}$ was also observed in already well-established words (i.e., "mature phase" in the life trajectory of words) [31], in which it appears in responses to noise and is related to the ultraslow diffusion dynamics (i.e., logarithmic diffusion).

5.3. Sequential parameter estimation and prediction

Forecasting is important for practical purposes. The forecasting task requires sequential parameter estimation, that is, parameter estimation at the intermediate points leading to a peak. We used the Bayesian estimation to make sequential parameter estimation. Details of the Bayesian estimation for the proposed model are provided in the Appendix A6. The time dependence of the posterior distribution of α, which describes the uncertainty of parameter estimation, is shown in Fig. 6 (e). Here, a prior distribution of α is assumed to have a uniform distribution from -2 to 2.

From Fig. 6 (e), we can see that at the initial time point ($0 \leq t \leq 20$), the posterior distribution also maintains a uniform distribution. This is because exponential growth at the beginning has no information about α. The predictions are shown in Fig. 6 (a), where the estimation is based on data before the grey vertical dotted line ($t = 27$). From the figure, it can be seen that the range of the predicted distribution shown by the green dashed line (from 1 percentile to 99 percentile) is very

broad.

Returning to Fig. 6 (e), for $t \sim 30$, the posterier distribution of α eliminates the possibility of $\alpha > 0$, and thereafter gradually converges to $\alpha \sim -0.5$ for $t \leq 30$. Based on the corresponding Figs. 6(b)-(d), we also confirm that the predicted posterior distribution becomes gradually narrower, i.e., more strongly predictable by the model. Note that for $Y > 0$, although the model can predict the growth process, the model cannot predict the time at the end of growth, T_j or $t_j^{(max)}$.

6. WEB SEARCH QUERY DATA

To confirm the generalizability of our study, we investigate web search query data (i.e., Google Trends). The details of Google Trends data are provided in subsection 2.2 in section 2.

Figs 2(a)-(d) show examples of comparisons between Google Trends (red crosses) and the blog data (black triangles). From Figs 2(a)-(c), we can confirm that the increase and decrease in the number of search queries are almost the same for the Japanese blog data. Although the time-series variation is common for many words, there are cases in which search queries differ from the blog data. For example, for the case of "SagamiharaShiTyuuouKu" (Sagamihara city central ward, new place name)", shown in the panel (d), the number of search queries increases abruptly when the place name is born (red crosses), while the number of blog articles increases linearly (black triangles). The hypotheses that explain this difference are as follows: (i) A person searches only once, when the person has recognized the replacement of the new place name with the old place; (ii) On the other hand, the person has permanently used and written the new place name in the blog many times after the recognition. To summarize the two hypotheses, From the macro perspective of society as a whole, the word counts in the blog data are linear because of the accumulation of random constant recognition (observed in search queries). Another example of a similar type of the difference is given in Fig. A1.

We compared the statistics of Google Trends data with blog data. Fig. 3(b) shows the valification of the proposed model given by Eq. 4 to search query data in English, French, Spanish, and Japanese, corresonpding analysis of Fig. 3(a) for the blog data in subsection 4.2 in section 4. The straight lines in this figure indicate that the model proposed by Eq. 4 is valid for all 4 languages statistically of Google Trends data.

Fig. 4(b) shows the distribution of the parameter α of the proposed model given by Eq. 4 for search query data. From Fig. 4(b), we can also confirm that the distributions of α for search query data (black triangles for Japanese, blue pluses for English, red circles for French and green crosses for Spanish) have peaks at $\alpha \sim -0.5$ and $\alpha \sim 1$ in the same as the Japanese blog data indicated by the yellow dashed line. Moreover, from panels (d) and (f), the distributions of Y and r for Google Trends data and the blog data also have almost the same shape density distributions.

These results imply that the model and statistical analysis in this study are probably valid not only for Japanese blog data but also for other languages and media. Note that the words studied in this research are not all words but rather article entries in Wikipedia, namely, words that have successfully spread in society to the level that they are published in online dictionaries.

7. CONCLUSION AND DISCUSSION

In this study, through systematic data analysis, we showed that the growth process of word counts of online can be well described by the slight extension of the logistic equation (Eq. 4) and is useful in analyzing online growth phenomena. First, the proposed model given by Eq. 4 can consistently describe the functional form of the growth curves observed by the actual time series data, such as the logistic function, the finite-time divergence, the linear function and the power-law function, etc., with two parameters α, Y essentially (Figs. 1, 3).

Second, we examined the statistics of the model parameters that reflect information on the dynamics of word-count time series. As a result, in the Japanese blog data, we found that the most typical values for the combination of parameters α and Y are $\alpha = -0.5$, $Y > 0$ (the word counts $y(t)$ asymptotical to the power-law function with exponent 2), or $\alpha = 1, Y < 0$ (corresponding to a logistic function or S-curve), as shown in Fig. 4. In addition, we also implied that parameter α is related to the subsequent peak after growth (Fig. 5).

Third, we analyzed search query data (i.e., Google Trends data) in English, French, Spanish and Japanese and we confirmed that the data had properties similar to the Japanese blog data (Fig. 3(b) and Fig. 4(b)).

Fourth, for forecasting applications, we attempted to predict parameters during growth using Bayesian statistics. As a result, we observed that the model parameters could not be limited owing to the wide range of possibilities in the early stages of growth, and after that the range of possibilities of parameters gradually narrowed down (Fig. 6). This implies that when forecasting using only the proposed model and the time series data, there are words that are difficult to forecast the time series in the early stages of growth, but then it becomes gradually predictable.

The limitations of the data are as follows:

- The focused words that have been included in the Wikipedia dictionary are not for all new words namely words that have successfully spread in society to the level that they are published in online dictionaries.

- Short-term growing words are out of the scope of the study (limited to words with a growth period

of at least one year).

- We used only online data and we don't use non-online words such as newspapers due to data acquisition limitations. However, the characteristics of the word-count time series may be common between online and non-online words, such as newspapers, because there are a lot of similarities in previous studies [31].

The limitations of this model are as follows:

- The proposed model cannot tell us anything about the micro-mechanisms although it restricts the macroscopic properties of the time series.

- The proposed model may still be redundant because parameter estimation is sometimes unstable without the regularization (see Appendix A5). Therefore, even as a macro model, there may be more essential time series models with fewer parameters than the proposed model.

The proposed model is not a first-principles model of growth dynamics in online languages but only an approximate model. However, even with an approximate model, we were able to show that a simple proposed model can systematically describe growth phenomena that appear superficially to be very diverse. In addition, by applying the proposed equation, we could analyze non-trivial mechanical properties. For example, we found that one of typical peak-out forgetting property $\propto \tau^{-0.5}$ is consistent with noise responses for well-established words observed in previous studies [31]. The coincidence in the aspects of two different forgetting phenomena, peak-out of new words and response to noise, may suggest the existence of a more universal dynamic property of social forgetting, whose entire picture has not yet been revealed. We hope that this research can contribute to the understanding of growth phenomena in society or in general complex systems, where diversity is one of the important factors.

Acknowledgments

The authors would like to thank Hottolink, Inc. for providing the data. This work was supported by JSPS KAKENHI, Grant Numbers 21K04529, 17K13815, and the Leading Initiative for Excellent Young Researchers MEXT Japan. We would like to thank Editage (www.editage.com) for English language editing. Computations were partially performed on the supercomputer system at ROIS Institute of statistical mathematics.

[1] P.-F. Verhulst, Correspondance Mathematique et Physique **10**, 113 (1838).
[2] J. S. Cramer, Tinbergen Institute Working Paper (2002).
[3] R. Pearl and L. J. Reed, Proceedings of the national academy of sciences **6**, 275 (1920).
[4] J. R. Skalski, K. E. Ryding, and J. Millspaugh, *Wildlife demography* (Academic Press, San Diego, CA, 2005).
[5] F. Hiroshi, K. Akemi, and M. Satoshi, Food Hygiene and Safety Science (Shokuhin Eiseigaku Zasshi) **44**, 155 (2003).
[6] R. A. Blythe and W. Croft, Language **88**, 269 (2012).
[7] D. Denison, Motives for language change **54**, 70 (2003).
[8] E. M. Rogers, *Diffusion of innovations* (Free Press, New York, NY, 2003).
[9] F. M. Bass, in *Winter Conference American Marketing Association* (American Marketing Association, Chicago,IL, 1963), pp. 269–275.
[10] K. Wu, D. Darcet, Q. Wang, and D. Sornette, Nonlinear dynamics **101**, 1561 (2020).
[11] V. Méndez, M. Assaf, D. Campos, and W. Horsthemke, Physical Review E **91**, 062133 (2015).
[12] S. H. Strogatz, *Nonlinear Dynamics and Chaos: With Applications to Physics, Biology, Chemistry, and Engineering, Second Edition* (Westview Press, New York, NY, 2018).
[13] F. Ghanbarnejad, M. Gerlach, J. M. Miotto, and E. G. Altmann, Journal of The Royal Society Interface **11**, 20141044 (2014).
[14] A. Piotrowskaja and R. Piotrowski, in *Statistika reci i avtomaticeskij analiz teksta*, edited by R. Piotrowski (Nauka, Leningrad, 1974), pp. 361–400.
[15] G. Altmann, H. von Buttlar, W. Rott, and U. Strauss, in *Historical Linguistics*, edited by B. Barron (Brockmeyer, Bochum, 1983), pp. 104–115.
[16] R. L. Górski and M. Eder, Journal of Quantitative Linguistics **30**, 125 (2023).
[17] J. Burridge and T. Blaxter, Journal of Physics: Complexity **2**, 035018 (2021).
[18] R. Amato, L. Lacasa, A. Díaz-Guilera, and A. Baronchelli, Proceedings of the National Academy of Sciences **115**, 8260 (2018).
[19] R. Maybaum, in *Annual Meeting of the Berkeley Linguistics Society* (Berkeley Linguistics Society, Berkeley Calif., 2013), No. 1, pp. 152–166.
[20] Google Trends, `https://trends.google.co.jp/trends`, 2022, (Accessed: 2022-11-22).
[21] F. S. Chapin, *Cultural change* (The Century Company, New York, NY, 1928).
[22] B. Ryan and N. C. Gross, Rural sociology **8**, 15 (1943).
[23] A. Brdulak, G. Chaberek, and J. Jagodziński, Energies **14**, 3216 (2021).
[24] E. G. Altmann and M. Gerlach, Physicists' papers on natural language from a complex systems viewpoint, `https://www.maths.usyd.edu.au/u/ega/physicist-language/`, 2019, (Accessed: 2022-11-28).
[25] D. M. Abrams and S. H. Strogatz, Nature **424**, 900 (2003).
[26] E. G. Altmann and M. Gerlach, in *Creativity and Universality in Language* (Springer International Publishing, Cham, 2016), pp. 7–26.
[27] A. M. Petersen *et al.*, Scientific reports **2**, 943 (2012).
[28] M. Gerlach and E. G. Altmann, Physical Review X **3**,

021006 (2013).
[29] J. Cong and H. Liu, Phys Life Rev. **11**, 598 (2014).
[30] H. Watanabe, Y. Sano, H. Takayasu, and M. Takayasu, Physical Review E **94**, 052317 (2016).
[31] H. Watanabe, Physical Review E **98**, 012308 (2018).
[32] H. Watanabe, The European Physical Journal B **94**, 227 (2021).
[33] M. Perc, Journal of The Royal Society Interface **9**, 3323 (2012).
[34] M. Perc, Scientific Reports **3**, 1720 (2013).
[35] Kuchikomi@kakaricho, `https://service.hottolink.co.jp/`, 2022, (Accessed: 2022-11-22).
[36] A. Ishii *et al.*, New journal of physics **14**, 063018 (2012).
[37] Y. Sano *et al.*, Phys. Rev. E **87**, 012805 (2013).
[38] Wikipedia:Database download, `https://en.wikipedia.org/wiki/Wikipedia:Database_download`, 2022, (Accessed: 2022-11-22).
[39] Analytics/AQS/Pageviews, `https://wikitech.wikimedia.org/wiki/Analytics/AQS/Pageviews`, 2022, (Accessed: 2022-11-22).
[40] V. Alfi, G. Parisi, and L. Pietronero, Nature Physics **3**, 746 (2007).
[41] R. J. Hyndman and Y. Khandakar, Journal of statistical software **27**, 1 (2008).
[42] S. J. Taylor and B. Letham, The American Statistician **72**, 37 (2018).
[43] C. M. Bishop, *Pattern recognition and machine learning* (Springer, New York, NY, 2006).
[44] K. Mullen *et al.*, Journal of Statistical Software **40**, 1 (2011).
[45] A. Perperoglou, W. Sauerbrei, M. Abrahamowicz, and M. Schmid, BMC medical research methodology **19**, 46 (2019).
[46] B. Carpenter *et al.*, Journal of statistical software **76**, 1 (2017).

Appendix

Appendix A1: Solutions of the extended logistic equation

We derived the solution to the extended logistic equation given in Eq. 4.

$$\frac{dy(t)}{dt} = ry(t)\left(1+\frac{y(t)}{Y}\right)^{\alpha} \tag{A1}$$

Using the separation of variables, we obtain

$$\frac{\frac{dy(t)}{dt}}{y(t)\left(1+\frac{y(t)}{N}\right)^{\alpha}} = r. \tag{A2}$$

By integrating both sides, we obtain

$$\int_{y(t_0)}^{y(t)} \frac{dy}{x\left(1+\frac{y}{Y}\right)^{\alpha}} = \int_{t_0}^{t} r dt. \tag{A3}$$

We solve with respect to t,

$$t = t_0 + \frac{1}{r}\int_{y(t_0)}^{y(t)} \frac{dy}{x\left(1+\frac{y}{Y}\right)^{\alpha}}. \tag{A4}$$

With the new variable, $v = 1 + y/N$,

$$\int_{y(t_0)}^{y(t)} \frac{dy}{y\left(1+\frac{y}{Y}\right)^{\alpha}} = \int_{1+y(t_0)/Y}^{1+y(t)/Y} \frac{dv}{(1-v)\,v^{\alpha}}. \tag{A5}$$

The following indefinite integral formula can be used

$$\int \frac{v^{-a}}{1-v}dv = \begin{cases} \frac{v^{1-a}\,{}_2F_1(a,1-a;2-a;v)}{1-a} & (others) \\ \frac{1-v}{|1-v|}\log(|1-v|)+\log(v) & (a=1) \\ \frac{1-v}{|1-v|}\log(|1-v|)+\log(v)+ & \\ \sum_{i=2}^{a}\frac{1}{-i+1}v^{-i+1} & (a=2,3,\cdots) \end{cases} + C, \tag{A6}$$

where ${}_2F_1(q_1,q_2;q_3;x)$ is a Gauss hypergeometric function, C is an arbitrary constant, and the second and third cases are derived from the partial fraction decomposition,

$$\frac{1}{(1-v)v^a} = \frac{1}{1-v} + \sum_{i=1}^{a}\frac{1}{v^i}. \tag{A7}$$

Using the function,

$$B_a(v) \equiv \begin{cases} \frac{v^{1-a}\,{}_2F_1(a,1-a;2-a;v)}{1-a} & (others) \\ \frac{1-v}{|1-v|}\log(|1-v|)+\log(v) & (a=1) \\ \frac{1-v}{|1-v|}\log(|1-v|)+\log(v) & \\ +\sum_{i=2}^{a}\frac{1}{-i+1}v^{-i+1} & (a=2,3,\cdots), \end{cases}$$

we can obtain

$$\int_{1+y(t_0)/N}^{1+y(t)/N} \frac{dv}{(1-v)\,v^{\alpha}} = B_\alpha(1+y(t)/Y) - B_\alpha(1+y(t_0)/Y). \tag{A8}$$

Therefore, we obtain the following solution,

$$t = t_0 + \frac{1}{r}(B_\alpha(1+y(t)/Y) - B_\alpha(1+y(t_0)/Y)). \tag{A9}$$

Formally solving for $y(t)$, $y(t)$ can be written as follows:

$$y(t) = Y\left(B_\alpha^{-1}(r(t-t_0)+b_0)-1\right). \tag{A10}$$

The expression $B_\alpha^{-1}(x)$ is the inverse function of $B_\alpha(x)$, $B_\alpha^{-1}(B_\alpha(x)) = x$, $0 < B_\alpha^{-1}(t) < 1$ for $Y < 0$, $B_\alpha^{-1}(t) > 1$ for $Y > 0$ and b_0 is defined by

$$b_0 = B_\alpha(1+y(t_0)/N). \tag{A11}$$

Appendix A2: Asymptotic properties of the model for $t \to \infty$

We compute four main categories of asymptotic properties of the extended logistic equation given by Eq. A1. Note that for $\alpha = 0$, which is not included in the four cases, we obtain the trivial solution $x(t) = y(t_0)\cdot\exp(r(t-t_0))$.

A2.1. $Y > 0$, $\alpha > 0$

Because $\frac{dy(t)}{dt} > 0$, $y(t)$ infinitely increases with no upper bound. Thus, for $y(t) \gg Y$, that is, $1 \ll \frac{y(t)}{Y}$, we can approximate Eq. A1 as follows:

$$\frac{dy(t)}{dt} = ry(t)\left(1+\frac{y(t)}{Y}\right)^{\alpha} \sim \frac{r}{Y^{\alpha}}y(t)^{\alpha+1} \tag{A1}$$

By solving this equation, we obtain

$$y(t) \approx \left(\frac{\alpha r(t_0-t)}{Y^{\alpha}} + y(t_0)^{-\alpha}\right)^{-1/\alpha}, \tag{A2}$$

where $y(t_0) \gg Y$. This equation diverges $y(t) \to \infty$ in finite time t^*,

$$t^* \approx t_0 + \frac{Y^{\alpha}}{\alpha r}y(t_0)^{-\alpha}. \tag{A3}$$

A2.2. $Y > 0$, $\alpha < 0$

From Eq. A2, for $\alpha < 0$, we can approximate Eq. A1 for $t \to \infty$ as follows:

$$y(t) \approx \left(\frac{|\alpha| r(t-t_0)}{Y^{\alpha}} + y(t_0)^{-\alpha}\right)^{1/|\alpha|}. \tag{A4}$$

By approximating this equation, we obtain the growth in the power law function

$$y(t) \propto t^{1/|\alpha|}. \tag{A5}$$

A2.3. $Y < 0$, $\alpha > 0$

For $Y < 0$, Eq. A1 is written by

$$\frac{dy(t)}{dt} = ry(t)\left(1 - \frac{y(t)}{|Y|}\right)^{\alpha}. \tag{A6}$$

As $\frac{dx(t)}{dt} = 0$ for $y(t) = |Y|$, $y(t)$ asymptotically approaches $y(t) = |Y|$ for $t \to \infty$. By rewriting the equation using $v(t)$, $v(t) = |Y| - y(t)$, we obtain

$$\frac{dv}{dt} = -r(|Y| - v)(v/|Y|)^{\alpha}. \tag{A7}$$

For $v(t) \ll 1$, Eq. A7 as follow:

$$\frac{dv}{dt} = -r|Y|^{1-\alpha}v^{\alpha}. \tag{A8}$$

Solving this equation for $\alpha \neq 1$ we obtain

$$v(t) = \left((\alpha - 1)r(t - t_0)|Y|^{1-\alpha} + v(t_0)^{1-\alpha}\right)^{1/(1-\alpha)}, \tag{A9}$$

and for $\alpha = 1$,

$$v(t) = v(t_0)\exp(r(t_0 - t)/|Y|). \tag{A10}$$

Thus, by turning back $y(t)$ from $v(t)$, for $\alpha \neq 1$,

$$y(t) \approx |Y|\left\{1 - \left((\alpha - 1)r(t - t_0) + (1 - y(t_0)/|Y|)^{1-\alpha}\right)^{1/(1-\alpha)}\right\}, \tag{A11}$$

and for $\alpha = 1$,

$$y(t) \approx |Y| - (N - y(t_0))\exp(r(t_0 - t)/|Y|). \tag{A12}$$

For $t \gg 1$ and $\alpha > 1$, Eq. A11 approaches Y asymptotically in the power law function of t,

$$y(t) \approx |Y|\left\{1 - ((\alpha - 1)rt)^{-1/(\alpha-1)}\right\}, \tag{A13}$$

and for $\alpha = 1$, Eq. A12 approaches Y asymptotically in the exponential law function of t,

$$y(t) \approx |Y| - (|Y| - y(t_0))\exp(r(t_0 - t)/|Y|), \tag{A14}$$

and for $0 < \alpha < 1$ Eq. A11 approaches Y in infinite time t^*,

$$y(t) \approx |Y| \cdot \left\{1 - \left((1 - y(t_0)/|Y|)^{1-\alpha} - (1 - \alpha)r(t - t_0)\right)^{1/(1-\alpha)}\right\}, \tag{A15}$$

where

$$t^* = t_0 + \frac{(|Y| - y(t_0))^{1-\alpha}}{r(1 - \alpha)|Y|^{1-\alpha}}. \tag{A16}$$

A2.4. $Y < 0$, $\alpha < 0$

From Eq 4, $\frac{dy(t)}{dt}$ diverges when $y(t^*) = Y$. t^* was determined using Eq. A16.

Appendix A3: Methodology for Sampling Words

The sampling of words for this study was based on the titles of Wikipedia articles. Note that because of this sampling, our study is limited to established enough to be the title of a Wikipedia article rather than temporary words that are quickly forgotten.

A3.1. Blog data

We extracted new words using the following steps. In step 1, we extracted the top one million words that had the highest frequency of articles in Japanese blog data from the list of titles in the Japanese version of Wikipedia [38]. In step 2, we filter out 20,764 words that had 0 blog entries in both November and December 2006 among the 1 million words.

A3.2. Google Trends

For Google Trends data, we employed Wikipedia page views to extract new words from all titles in the English, French, and Spanish editions of Wikipedia [38]. First, we collected page view data for the first day of each month from May 2015 through January 2022. Next, we extracted new words such that the word had 0 page views on May 1, 2015 (i.e., the first month of observation) and 50 or more views (French, Spanish and Japanese) or 1,000 or more views (English) on January 1 of 2016, 2017, $\cdots$, 2021 or 2022. Finally, we used the Google Trends API to obtain Google Trends for selected words [20].

Appendix A4: Methodology for Extracting an uptrend

Here, we show how we extracted a global growth period that is not a temporary local trend. The example of the global growth period is the period enclosed by the grey vertical lines in Fig. 2. First, we describe the detection of the starting point of growth and next the detection of the end point of growth.

A4.1. Extracting the beginning of growth

Basically, the starting point of the growth trend t_0^s is the minimum point of the 13-points moving median time series or the minimum point of corresponding row time

series, $t_0^s = \max(t_1^s, t_2^s)$, where the minimum of the 13-points moving median of word counts $y_j(t)$ is denoted as $t_1^s = argmin_t\{MovingMedian_{13}(y_j(t))\}$ and the minimum of corresponding row time series is denoted as $t_2^s = argmin_t\{MovingMedian_{13}(y_j(t))\}$ and $y_j(t) = 0$ is excluded. More precisely, the following procedure was used to determine the starting point of the growth:

1. We calculate the upper limit of candidates, T^s. The upper limit is set so that 13-points moving median first reaches the 25th percentile point, $T^s = min_t\{t|y(t) \geq Quantile25\{y(t)\}\}$. This procedure is introduced to avoid selecting minimum points during a downtrend after an uptrend.

2. We calculate the first candidate of the starting point t_1^s. The first candidate is set as the time such that the 13-points moving median time series is minimum $t_1^s = argmin_{\{t \leq T_s\}}\{MovingMedian_{13}(y_j(t))\}$. Here, the minimum value is less than 10, we recalculate using the 13-points moving median time series that is not normalized by the total number of articles $MovingMedian_{13}(x_j(t))$, where $x_j(t)$ is raw time series defined in the section 2.

3. We calculate the second candidate of starting point t_2^s. This second candidate is set as the time such that the raw time series (i.e., not taking the moving median) is the smallest and is calculated $t_2^s = argmin_{\{t \leq T_s\}}\{y_j(t)\}$. Here, if the smallest value of the time series is less than 10, so we recalculate using the time series not normalized by the total number of articles $x_j(t)$.

4. We determine the starting point of growth t_0^s. Basically, we chose the starting point of the trend as the larger time of the two candidate points, conservatively, $t_0^s = \max(t_1^s, t_2^s)$. However, if there is a clear upward trend between the two candidates $\{t_1^s, t_2^s\}$, we set the starting point t_0^s as the smaller time $t_0^s = \min(t_1^s, t_2^s)$ is selected as the growth starting point (The trend is identified based on the positive rank correlation between times $\{\min(t_1^s, t_2^s), \min(t_1^s, t_2^s) + 1, \cdots, \max(t_1^s, t_2^s)\}$ and the corresponding counts $\{y_j(min(t_1^s, t_2^s)), y_j(min(t_1^s, t_2^s) + 1) \cdots y_j(max(t_1^s, t_2^s))\}$. Here, we recognize the trend when a p-value is less than 0.01 for the test of correlation.).

A4.2. Extraction of end of growth

Basically, the endpoint of growth, t_0^e, is detected as the point at which a clear downward trend begins. A clear downward trend is defined as a continuous decrease in word count for at least 12 months after the starting point ($t_0^s \leq t_0^e$). Specifically, we first roughly search for the starting point of the downtrend at the 13-points moving median to avoid being fooled by local trends. Next, we improve candidate points using progressively smaller time scale information (5-points moving median, 3-points median and original data). Finally, we examine whether the starting point of the downtrends found by the above method or the global maximum point is more suitable as the endpoint of the global uptrend. The details of the procedure are as follows:

1. Detecting the starting points of a clear downtrend for the 13-points moving median t_1^e. Specifically, we select the point such that the starting point is where the 13-points moving median of the time series falls continuously for at least 12 time-points consecutively (i.e., approximately 12 months or a year). Here, to avoid the error of detecting local downtrends, the start of a downtrend is detected at a point after the point at which the time series reaches the 90th percentile $T^e = min_t\{t|y(t) \geq Quantile90\{y(t)\}\}$, namely, we choose $t_1^e > T^e$. If there is no point at which there are 12 consecutive downtrends, the last point of observation is taken as the end point of growth, $t_1^e = T$.

2. Exploring around the t_1^e. To determine the end of the growth trend more precisely, we explore in more detail the area around the t_1^e which calculated the previous step. Specifically, in this step, we make several other candidates set for the end time of the growth trend $\{t_2^e\}$. The candidates in the set $\{t_2^e\}$ satisfy the following condition: the 13-points moving median is greater than 90% of the maximum value between t_0^s and t_1^f. Particularly we calculate the set of candidates,

$$\{t_2^f\} = \{t|t_0^s \leq t \leq t_1^e, MovingMedian_{13}(y(t)) \geq 0.9 \times \max_{\{t_0^s \leq t \leq t_1^e\}}(MovingMdedian_{13}(y(t)))\}.$$

3. Adding information about shorter time scales (5-points moving median). For all candidate points $\{t_2^e\}$, we search the neighbourhoods and replace the point such that point is reached by continuously increasing in 5-points moving median. Particularly, for all candidate points $t \in \{t_2^e\}$, we replace $t \to t^*$ using the following formula,

$$\begin{aligned} t_0^* &= t_0 + argmax_{\{t \in \{t_0+m^-, t_0+m^+\}\}}(q_j(t)) \quad \text{(A1)} \\ m^+ &= \max(\{m|m, s \in \mathbb{N}, m \geq 0, 0 \leq s \leq m \\ &\quad , \forall s[q_j(t_0+s) \leq q_j(t_0+s+1)]\}) \\ m^- &= \min(\{m|m, s \in \mathbb{N}, m \leq 0, m \leq s \leq 0, \\ &\quad \forall s[q_j(t_0+s) \leq q_j(t_0+s-1)]\}). \end{aligned}$$

Here, we use the $q_j(t) = MovingMedian_5(f_j(t))$, $\{t_0\} \to \{t_2^e\}$ and $\{t_0^*\} \to \{t_3^e\}$. This transformation corresponds to a correction for the candidate points in the 13-points moving median with the addition

of information on a shorter time scale (i.e., the 5-points moving median).

4. Adding information of 3-points moving median. Next, a similar to previous step's transform process given by Eq. A1 is performed for the 3-points moving median, $q_j(t) = MovingMedian_3(f_j(t))$, with the starting point of this process being the candidate point in the 5-points moving median, $\{t_3^e\}$ calculated in the previous step, $\{t_0\} \to \{t_3^e\}$. The candidate point using the 3-points moving median is calculated as $\{t_0^*\} \to \{t_4^e\}$.

5. We determine the tentative end point of the growth trend, t_5^e. The end time of the growth trend is determined by the point with the largest number of growth trend candidate points $t_5^e = argmax_{t\in\{t_4^e\}}(MovingMedian_3(y_j(t)))$.

6. Fine-tuning with raw data (adding information of raw data). We use raw data (data without a moving median) $y_j(t)$ to fine-tune the end points of the growth trend. Specifically, we change the candidate point to a larger point near the candidate point determined by Eq. A1 for $q_j(t) = f_j(t)$ and $t_0 \to t_5^f$. We denote the transformed time as $t_6^e = t_5^e + argmax_{\{t\in\{t_5^e+m^-,t_5^e+m^+\}\}}(y_j(t))$.

7. Comparison between the candidate t_6^e and the global maximum point $t^{max} = argmax_t[y_j(t)]$. In cases where there is a maximum in the whole time series at 6 points before or after the candidate point (i.e., the case t^{max} is satisfied with $t_6^e - 6 \le t^{max} \le t_6^e + 6$), we check whether the maximum of the data t^{max} is more suitable as the end point of the growth trend than the current candidate point t_6^e. Specifically, we make sure that the maximum is not a temporary maximum due to news or external forces or there is a clear upward trend from the candidate point to the maximum point. A clear uptrend is defined as a time series extracted between the candidate points t_6^e and the maximum point t^{max}, $\{y(\min(t_6^e, t^{max})), y(\min(t_6^e, t^{max}) + 1), \cdots, y(\max(t_6^e, t^{max}))\}$ that satisfies either of the following three conditions: (i) A linear approximation is well fitted, and the regression coefficient is not zero (coefficient of determination is greater than 0.4, the sign of the regression coefficient is $sign(t^{(max)} - t_6^e)$ and the p-value of the coefficient is less than 1%). (ii) A good fit of the approximation to a quadratic function (coefficient of determination greater than or equal to 0.85) and the function's differential is always positive in the focus period for $t_6^e < t^{max}$ or always negative for $t^{max} < t_6^e$. (iii)The binomial test of differential for the positive ratio for $t_6^e < t^{max}$ or negative ratio for $t^{max} < t_6^e$ taking 0.6 (the one-sided test p-value of the coefficient is less than 5%). If the conditions are satisfied, the final candidate point is $t_0^e = t^{max}$. If the condition is not satisfied, then $t_0^e = t_6^e$.

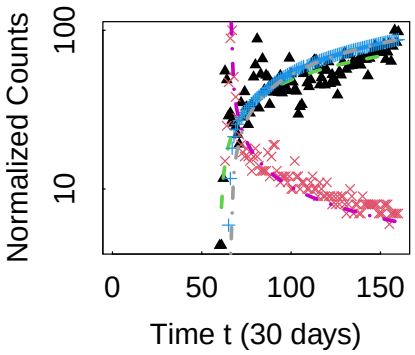


FIG. A1: Comparison of time series between blog data (black triangles) and Google Trends (red crosses) for "Toyota·Akua" (Toyota Aqua, Name of a car, $\alpha = -2.56, Y = 15.7, r = 16.8, y(0) = 4.47$). Blog data is scaled to a maximum value of 100. The green dashed line indicates the theoretical curve given by the model Eq. 4. The gray dash-dotted line is power-law function $\propto t^{0.5}$, purple red dash-dotted line is power-law function $\propto t^{-0.5}$ and green pluses represent scaled cumulative values of Google Trends. From the figure, we can confirm that the blog data corresponds well to the cumulative values of Google Trends.

Appendix A5: Estimation of Parameters

We determined the parameters r, α, and Y to minimize the following median absolute error: A regularization term (lasso or least absolute shrinkage and selection operator) is added to stabilize the estimation [43].

$$Median_{\{t=1,2,\cdots,T_j\}}[y_j(t) - F(t|\alpha, r, Y))] + \lambda(|r| + |Y|), \tag{A1}$$

where the solution to $\frac{dy(t)}{dt} = f(t|\alpha, r, Y)$ is denoted by $y(t) = F(t|\alpha, r, Y)$ (in the case of the proposed model, $f(t|\alpha, r, Y)$ is given by Eq.A1 and $F(t|\alpha, r, Y)$ is given by A10). In this study, we employ a differential evolution algorithm for global optimization and $\lambda = 0.03$ [44]. The initial state $y(0)$ is determined by the initial value $\bar{y}(t_0)$ of the time series of smoothed splines $y(t)$ (in the case of $\bar{y}(t_0) < 0$, we use $y(t_0) = 0.8$) [45].

Note that for $\alpha > 0$ and $y(t) \gg Y > 0$, the proposed model can be approximated by

$$\frac{dy(t)}{dt} = ry(t)\left(1 - \frac{y(t)}{Y}\right) \approx \frac{r}{Y^\alpha} y(t)^{\alpha+1} = Cy(t)^{\alpha+1}, \tag{A2}$$

where $C = \frac{r}{Y^\alpha}$ is the constant. The equation shows that r and Y are not uniquely determined. This indeterminacy may be one reason why estimation is unstable without regularization.

Appendix A6: Parameter Estimation with Bayesian Statistics

To perform the estimation using Bayesian statistics, we extended the model given by Eq. A1 to a stochastic model. Specifically, we add independent noise $y(t;\alpha,Y,r)\epsilon(t|\sigma)$ with a normal distribution whose standard deviation is proportional to $y(t)$,

$$\tilde{y}(t|\alpha,Y,r,\sigma) = y(t;\alpha,Y,r) + y(t;\alpha,Y,r)\cdot\epsilon(t|\sigma) \quad \text{(A1)}$$

Here, $y(t;\alpha,Y,r)$ is calculated by Eq. A10 or Eq .A1 and the noise $\epsilon(t|\sigma)$ is a normal distribution with a mean of 0 and standard deviation σ,

$$\epsilon(t|\sigma) \sim Norm(0,\sigma). \quad \text{(A2)}$$

$$\text{(A3)}$$

For the convergence of the Bayesian estimation, we use the following prior distributions: The prior distributions of parameters r and σ are uniform distributions

$$r \sim Unif(0,1.5) \quad \text{(A4)}$$

$$\sigma \sim Unif(0,0.2), \quad \text{(A5)}$$

$$\text{(A6)}$$

where $Unif(a,b)$ denotes a uniform distribution that takes values from a to b. The prior distribution of α is asymmetric and uniform.

$$\alpha|q \sim AcymetricUnif(-2,0;q), \quad \text{(A7)}$$

$$\text{(A8)}$$

Here, the probability density distribution of the asymmetric uniform distribution is defined as

$$p(\alpha|q) = \begin{cases} q/2 & (0 \le \alpha \le 2) \\ (1-q)/2 & (-2 \le \alpha \le 0) \\ 0 & (otherwise), \end{cases} \quad \text{(A9)}$$

where the prior distribution of q is given by a uniform distribution,

$$q \sim Unif(0,1). \quad \text{(A10)}$$

This distribution is a mixture of $Unif(0,2)$ and $Unif(-2,0)$ with a mixing ratio parameter of $0 \le q \le 1$. This mixed distribution was introduced to prevent the Markov chain Monte Carlo method (a method for estimating parameters) from falling into a local solution. Without this distribution, α is likely to fall into either a positive or negative local solution because the likelihood around $\alpha \approx 0$ is often very low.

Finally, we employ the following mixture two-sided exponential distribution as a prior distribution for Y,

$$Y|\alpha \sim \begin{cases} DoubleExponential(0,10^6) & (\alpha \ge 0) \\ AcymetricDoubleExpnential(0,10^6;0.95) & (\alpha < 0) \end{cases} \quad \text{(A11)}$$

where the probability density distribution of this prior distribution is given by

$$P(Y|\alpha) = \begin{cases} \frac{1}{2\mu}\cdot\exp(-|Y|/\mu) & (\alpha \ge 0) \\ \frac{0.95}{2\mu}\cdot\exp(-|Y|/\mu) & (\alpha < 0, Y > 0) \\ \frac{0.05}{2\mu}\cdot\exp(-|Y|/\mu) & (\alpha < 0, Y < 0), \end{cases} \quad \text{(A12)}$$

and $\mu \sim Unif(0,10^6)$. This prior distribution is introduced for two reasons: (i) Y is as close to 0 as possible if not necessary (Bayesian lasso) and (ii) prior information that few words have $\alpha < 0$ and $Y < 0$ (see Table II).

We compute the posterior distribution of $y(t)$ using the Hamiltonian Monte Carlo method with the computer library "Stan" [46].

Appendix A7: Comparison of models

We compared the proposed model given by Eq. 4 with other models related to the logistic equation.

A7.1. Two parmeter model

First, we discuss the two-parameter models, which are special cases of the proposed model given by Eq. A1. We check the following models.

- (a) The logistic equation:

$$\frac{dy_j(t)}{dt} = r_j y_j(t)\left(1 - y_j(t)/Y_j\right), \quad \text{(A1)}$$

  where $Y_j > 0$. This is the basic logistic equation and the special case of the proposed model given by Eq. A1 for $\alpha = 1$ and $Y < 0$.

- (b) Y-sign extended logistic equation:

$$\frac{dy_j(t)}{dt} = r_j y_j(t)\left(1 + y_j(t)/Y_j\right), \quad \text{(A2)}$$

  where $Y_j \neq 0$. This equation extends the logistic equation to the carrying capacity Y_j taking the positive and negative sign. In the case that $Y_j < 0$, the equation corresponds to the basic logistic equation given by Eq. A1; and the special case of the proposed model given by Eq. A1 for $\alpha = 1$.

- (c) Single factor power-law model:

$$\frac{dy_j(t)}{dt} = r_j \cdot y_j(t)^{\alpha_j+1}. \quad \text{(A3)}$$

  This equation is a simple power-law type differential equation, corresponding to the proposed model given by Eq. A1 for $Y \gg 1$.

Figs. A2(a)-(c) show a direct validation of the differential equations of above-mentioned models given by Eqs. A1, A2 and A3. The x-axis corresponds to the right-hand side of the model, and the y-axis corresponds to the left-hand side. Thus, the closer the plotted curve is to the line $y = x$, as shown by the red dashed line, the better the correspondence with the models. Here, to take the statistics regarding the words j, we use quantities normalized by the scale parameter Y_j, $p_j(t) = \frac{dy_j(t)}{dt}/|Y_j|$ in the y-axis and $q_j(t) = f(y_j(t)|\alpha_j, r_j, Y_j)/|Y_j|$ in the x-axis, where the differential equation is denoted as $\frac{dy}{dt} = f(y)$. If a model can explain the data, the graph remains linear after scale transformation.

More specifically, to make Fig. A2, we calculate the following values. First, for the x-axis, the scaled right-hand side of the model is calculated as

$$p_j(t) = f(y_j(t)|\alpha_j, r_j, Y_j)/|Y_j|, \tag{A4}$$

where the differential equation is denoted by $\frac{dy}{dt} = f(y|\alpha, r, Y)$ and the model parameters are Y, r, α are estimated by minimizing Eq.A1 in Appendix A5 .

Second, for the y-axis, we approximate the derivative on the left-hand side of the models using the difference,

$$q_j(t) = \frac{1}{|Y_j|} \cdot (MovingMedian_3(y_j(t+1)) - MovingMedian_3(y_j(t))), \tag{A5}$$

where the moving median of the three points is used to remove noise from the time series.

Finally, to create a graph, we introduce an ensemble median for t and j conditioned on α_j^0 and $s_j^{(0)}$,

$$\hat{q}(p|\alpha_j^{(0)}, s^{(0)}) = Median_{\{j,t|, d_p^- < p_j(t) < d_p^+, |\alpha_j^{(0)} - \alpha| < d_\alpha, sign(Y_j) = s_j^{(0)}\}}[q_j'(t))], \tag{A6}$$

where $d_\alpha = 0.5$ for $Y > 0$ or $d_\alpha = \infty$ for $Y < 0$ is the box size of α to obtain the statistics, $d_p^+ = p(\exp(0.1))$, $d_p^- = p(\exp(-0.1))$ is the box size of p, α_j^0, $s_j^{(0)} = sign(Y_j^{(0)})$, $Y_j^{(0)}$ are the parameters of j-th word of the proposed model given by Eq. A1. For this calculation, in the case of the single factor power-law model given by Eq. A3, we use $Y_j = Y_j^{(0)}$ for scaling in Eq. A4 and A5 because the model does not have the scale parameter Y_j.

In Fig. A2, we plot $\hat{q}(p|\alpha_j^{(0)}, s^{(0)})$ as a function of p, with p on the x-axis and $\hat{q}$ on the y-axis. The black triangle is the statistic for all data, whereas the other colors and shapes are medians conditioned on $\alpha^{(0)}$ or $Y^{(0)}$.

For the logistic equations given in Eq. A1 shown in Fig. A2(a) and the sign-extended logistic equation given by Eq. A2 shown in Fig. A2(b), for small p, the data are almost consistent with the theoretical line $\hat{q} = p$, but for large p they are not. The reason for the disagreement with theory is that these models cannot represent the growth functions of the powers of t such as $y_j(t) \propto t$ and $y_j(t) \propto t^2$.

Conversely, in the single factor power-law model given by Eq. A3, for the large p, the statistics for the whole data, indicated by the black triangle, correspond to the theoretical line $\hat{q} = p$ (except for the largest outliers), but not for the small p. Furthermore, the figure also confirms that the model cannot be explained by the growth curve for $Y^{(0)} < 0$ (i.e., S-shaped or logistic-like curve) indicated by the peach crosses. The reason for the disagreement with theory is that the single factor power-law model cannot represent the growth curve, which asymptotically converges to a constant value. $y_j(t) = const$ for $t \gg 1$.

The proposed model given by Eq. 4 or A1 is a combination of the (sign-extended) logistic equation (Eq. A2) and the single factor power-law model (Eq. A3). For $Y > 0$ and $y_j(t) \gg |Y|$, the model can be approximated as the single factor power-law model, and where $y(t) \ll |Y|$ is small or $Y < 0$, it behaves like the logistic equation.

A7.2. Three parmeter model I (Linear extension)

Next, we examine the three-parameter models. First, we check the Bass model and a model with a constant term, which are typical extensions of the logistic equation:

- (d) Bass model (Y-sign extended):

$$\frac{dy_j(t)}{dt} = (r_j y_j(t) + \alpha_j)\,(1 + y_j(t)/Y_j)\,, \tag{A7}$$

  where $\alpha_j > 0$ and $Y_j \neq 0$.

- (e) Constant term model:

$$\frac{dy_j(t)}{dt} = r_j y_j(t)\,(1 + y_j(t)/Y_j) + \alpha_j, \tag{A8}$$

  where $\alpha_j > 0$ and $Y_j \neq 0$.

The points in Figs. A2(d) and (e) are not straight lines. Thus, we can confirm that these extensions are not effective in explaining the data.

A7.3. Three parmeter model II (Power-law extension)

We discuss the three-parameter model with the power-law factor, which is a special case of the (Y-sign extended) Blumberg equation or the (Y-sign extended) generalized logistic equation [10]. Note that, while the original models are for $Y_j < 0$, in this study, it is extended to $Y_j \neq 0$.

- (f) First factor power-law model:

$$\frac{dy_j(t)}{dt} = r_j y_j(t)^{\alpha_j} \left(1 + y_j(t)/Y_j\right), \tag{A9}$$

where $Y_j \neq 0$ and α_j take both negative and positive real numbers. We call this model a "First factor power-law model" because the model has the power term in the first factor.

- (g) Second factor power-law model (Proposed model):

$$\frac{dy_j(t)}{dt} = r_j y_j(t) \left(1 + y_j(t)/Y_j\right)^{\alpha_j}, \tag{A10}$$

where $Y_j \neq 0$ and α_j take both negative and positive real numbers. We call this model a "Second factor power-law model" or "Proposed model" because the model has the power term in the second factor and corresponds proposed model given by Eq. A1.

- (h) Inside power-law model (Y-sign extended Richards' Equation):

$$\frac{dy_j(t)}{dt} = r_j y_j(t) \left(1 + sign(Y_j) \cdot (y_j(t)/|Y_j|)^{\alpha_j}\right) \tag{A11}$$

where $Y_j \neq 0$ and α_j takes both negative and positive real number. We call this model as "Inside power-law model" because the model has the power term inside the second factor.

From Figs. A2 (f) and (g) for the first factor power-law model given by Eq. A9 and the second factor power-law model given by Eq. A10, the data agree well with the theoretical straight line $p = q$. The results imply that these models are not inconsistent with real growth dynamics.

We were unable to provide conclusive evidence of the difference between the first factor power-law model (f) and the second factor power-law model (g) in our data analysis. Therefore, we adopted the second factor power-law model, given by Eq. A10 as the proposed model for the following reasons:

- The second factor power-law model (the proposed model) had better predictive ability than the first factor power-law model given in table A1.

- The proposed model is consistent with the data analysis results of the two-parameter models, and the relationship with those two-parameter models is easy to interpret (see Appendix in section A7.1.

From Fig. A2(f) we can see that the inside power-law model given by Eq. A11 deviates from the theoretical line. One reason may be that this model cannot explain the growth curve of the power asymptote for $\alpha^{(0)} < 0$, such as $y(t) \propto t$.

A7.4. Confirmation of the sign effect of the proposed model

Finally, we verified the sign-restricted version of the proposed model,

- (i) Y-sign positive-restricted second factor power-law model (Positive model):

$$\frac{dy_j(t)}{dt} = r_j y_j(t) \left(1 + y_j(t)/Y_j\right)^{\alpha_j}, \tag{A12}$$

where $Y_j > 0$. This model corresponds to the proposed model (Eq. A10) restricted to $Y_j > 0$.

- (j) Y-sign negative-restricted second factor power-law model (Negative model):

$$\frac{dy_j(t)}{dt} = r_j y_j(t) \left(1 + y_j(t)/Y_j\right)^{\alpha_j}, \tag{A13}$$

where $Y_j < 0$. This model corresponds to the proposed model (Eq. A10) restricted to $Y_j < 0$.

In Fig. A2 (i), for the model restricted to $Y_j > 0$ given by Eq. A12, the curve is linear and does not clearly differ from the proposed model. However, Fig. A4(i) also indicates that this model does not explain the actual data better than the proposed model (The detail is mentioned in the section A7.5). When restricted to $Y < 0$, as expressed by Eq. A13, the model shows that it cannot explain the data (see Fig. A2(j)). This is because the model can only represent the growth curves of the S-shape type.

These results imply that the proposed model can explain the growth curve relatively well, even when restricted to $Y > 0$ (but does not explain the S-shape type curves).

A7.5. Comparisons using other statistics

We discuss theoretical relationships that are not differential equations as discussed in the previous section (Fig .A2). In particular, we use the relation of the raw time $t_j = F^{(-1)}(y_j|\alpha_j, r_j, Y_j)$ in Fig. A3, scaled time $t_j/T_j = F^{(-1)}(y_j|\alpha_j, r_j, Y_j)/T_j$ in Fig. A4, and the scaled word counts $y_j/Y_j = F(t_j|\alpha_j, r_j, Y_j)/Y_j$ in Fig. A5, where the solution of $\frac{dy(t)}{dt} = f(t|\alpha, r, Y)$ is denoted as $y(t) = F(t|\alpha, r, Y)$, its inverse function is denoted as $t = F^{(-1)}(y(t)|\alpha, r, Y)$ and T_j is the length of the growth period of j-th word. In these figures, we plotted the ensemble median values in the same way as in Eq. A6

From these figures, it can be seen that both the first factor power-law model given in Eq. A9 shown in the panel (f) and the second factor power-law model (the proposed model) given by Eq. A10 shown in the panel (g) can explain the real data consistently.

Note that in Fig. A4 (g), for the small p, even the proposed model cannot explain well the growth curve

of the finite-time divergence (i.e., $\alpha^{(0)} > 0, Y^{(0)} > 0$) shown in green points. The reason is expected to be that the curve of finite-time divergence grows very slowly at the beginning; therefore, it is difficult to distinguish the growth dynamics from noise for a small p. Thus, the subsequent stagnation for small p in Fig. A4 (g) is considered stagnation until the growth dynamics of the model exceed the noise level.

Although in Fig. A2 we could not distinguish between the proposed model shown in panel (g) and the positive model shown in panel (i), we can distinguished these models in Fig. A4. In particular, as shown in Figs. A4 (i) the positive model given by Eq .A12 can not explain the growth curve of the S-curve ($Y^{(0)} < 0$) shown in magenta crosses.

The specific calculations used in Figs A3, A4 and A5, respectively, are as follows: We replace $p_j(t)$ as given in Eq. A4 and $q_j(t)$ given in Eq. A5 with the following quantities, in Fig. A3, we use the time t,

$$p_j(t) = F^{(-1)}(y_j(t)|Y_j, r_j, \alpha_j), \tag{A14}$$

$$q_j(t) = t, \tag{A15}$$

in Fig. A4 we use the scaled time t,

$$p_j(t) = F^{(-1)}(y_j(t)|Y_j, r_j, \alpha_j)/T_j, \tag{A16}$$

$$q_j(t) = t/T_j, \tag{A17}$$

and in Fig. A5, we use scaled word count y,

$$p_j(t) = F(y_j(t)|Y_j, r_j, \alpha_j)/|Y_j|, \tag{A18}$$

$$q_j(t) = y_j(t)/|Y_j|. \tag{A19}$$

A7.6. Comparison of forecasting ability between models

We compared the forecasting ability of the models introduced in section A7. Specifically, we estimated the model parameters using the first 70 percent of the time series from the beginning of the growth period and predicted the remaining 30 percent of the time series. As the same way as Eq. 19 in subsection 4.3 in section 4, the absolute mean error was used as a measure of fit to the data,

$$\delta_j^{(model)} = Mean_{\{t|0.70T_j \le t \le T_j\}}[F^{(model)}(t|\alpha_j, r_j, Y_j) - y_j(t)|], \tag{A20}$$

where $F^{(model)}(t|\alpha_j, r_j, Y_j)$ is the solution of models, such as the logarithmic equation given by Eq. A1 and the negative model given by Eq .A13. Table A1 shows the winning ratio of the proposed model (i.e., the number ratio of the word-count time series for which the proposed model has a higher prediction accuracy than the comparison model). As the same way as Eq. 21, the winning ratio against the proposed model is defined as

$$R^{(model)} = \frac{\sum_{\{j|\delta_j^{(model)} > \delta_j^{(0)}, i \in W_s\}} 1}{\sum_{\{i|\delta_j^{(model)} > \delta_j^{(0)}, j \in W_s\}} 1 + \sum_{\{i|\delta_j^{(model)} < \delta_j^{(0)}, j \in W_s\}} 1}, \tag{A21}$$

where we estimated the parameters of each word using data from $t = 1$ to $t = 0.7 \times T_j$.

In this table, we also show the winning ratio for training errors using all data.

$$S^{(model)} = \frac{\sum_{\{j|\Delta_j^{(model)} > \Delta_j^{(0)}, j \in W_s\}} 1}{\sum_{\{j|\Delta_j^{(model)} > \Delta_j^{(0)}, i \in W_s\}} 1 + \sum_{\{j|\Delta_j^{(model)} < \Delta_j^{(0)}, j \in W_s\}} 1}, \tag{A22}$$

where the training error is defined as:

$$\Delta_j = Mean_{\{t|1 \le t \le T_j\}}[|F^{(model)}(t|\alpha_j, r_j, Y_j) - y_j(t)|], \tag{A23}$$

where we estimated the parameters of each word using data from $t = 1$ to $t = T_j$.

In addition to the models (a)-(g) mentioned in section A7, we added the SARIMA model and Prophet model to the table A1.

From the table, we can see that the proposed model is relatively more accurate than the compared models in terms of prediction error R except for the single power-law model (c) and the positive model (i). The reason for these exceptions is probably that the two models (c) and (i) remove the $Y < 0$ region from the parameter estimation and it prevents overfitting. Since the frequency of the words with $Y < 0$ is small (see table II), negative effects of this limitation of $Y > 0$ on the winning ratio R can be expected to be relatively small. We can also see from the table that the proposed model is as accurate or more accurate than the compared models in terms of the training error S except for some models. Here, we discuss the reasons for the exceptions: (i) For the Prophet model $S^{(Prophet)} = 0.34 < 0.5$, the result that the predictive ability is not as good as that of the proposed model, $R^{(Prophet)} = 0.59 > 0.5$ suggests overfitting, and (ii) for the inside power-law model, taking $S^{(Inside)} = 0.39 < 0.5$, it is unclear why the model has more explanatory power for training than that of the proposed model.

Note that because the proposed model includes the logistic model as a special case, $S^{(logistic)}$ should take 1 theoretically, but in reality, $S^{(logistic)} \approx 0.85$. The reason for this is the limitation of the numerical optimization performed in this study, which does not yield a theoretically perfect minimum solution.

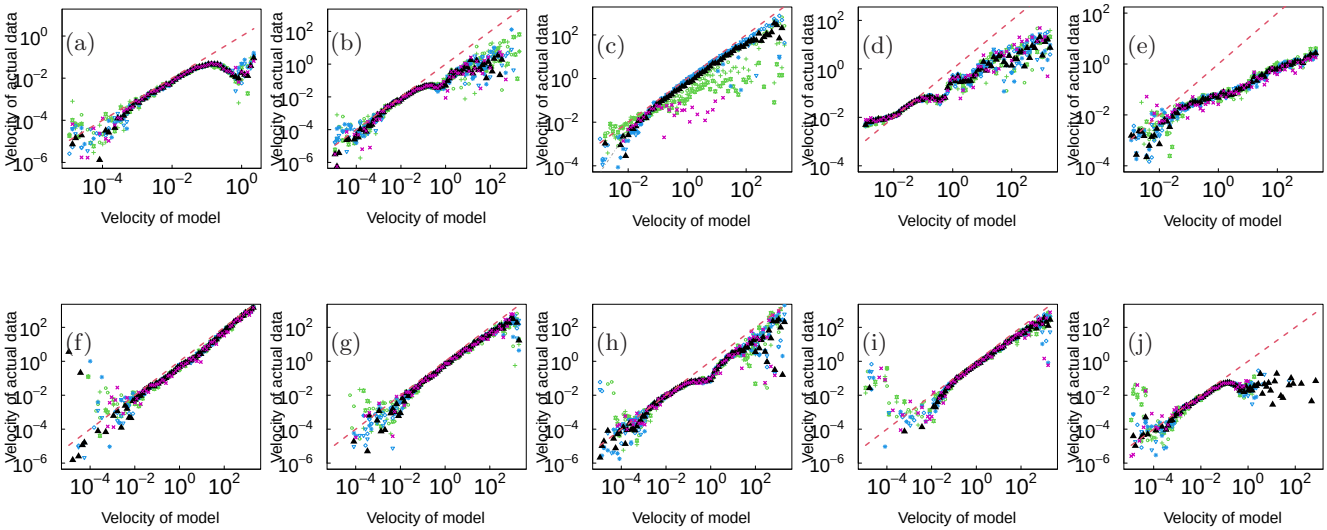


FIG. A2: Comparison of models given in Appendix A7 by using the differential equations. If the model explains the data well, the graph will be close to the $y = x$ line shown by the red dashed line. The y-axis corresponds to the left-hand side, $dy(t)/(dt) \cdot 1/|Y|$ of a model and the x-axis to the right-hand side $f(y_j(t)|\alpha, Y)/|Y|$ of a model, where a model is written by a differential equation, $\frac{dy(t)}{dt} = f(y(t)|\alpha, Y)$. Specifically, we plot the median quantity with respect to words given by Eq. A6, which is scaled by the model's scale parameter Y. The ensemble median over all data is plotted in black triangles and also the ensemble median grouped by proposed model's (Eq. A1) parameters $\alpha_j^{(0)}$ and $Y_j^{(0)}$ is plotted. In case of $Y_j^{(0)} > 0$, we plott in green circles for $\alpha_j^{(0)} = 0.5$, green pluses for $\alpha_j^{(0)} = 1.0$, for green triangles up and down $\alpha_j^{(0)} = 1.5$, blue diamonds for $\alpha_j^{(0)} = -0.5$, blue triangles point down for $\alpha_j^{(0)} = -1.0$ and in the case of $Y_j^{(0)} < 0$ magenta corsses. (a) Logistic equation given by Eq. A1, (b) Y-sign extended logistic equation given by Eq. A2, (c) Single factor power-law model given by Eq. A3, (d)(Y-sign extended) Bass model given by Eq. A7, (e) Constant model given by Eq. A8, (f) First factor power-law model given by Eq. A9, (g) Second factor power-law model (Proposed model) given by Eq. A10, (h) Inside power-law model given by Eq. A11, (i) Y-sign positive-restricted second factor power-law model given by Eq. A12 and (j)Y-sign negative-restricted second factor power-law model given by Eq. A13.

Appendix A8: Examples of words in the four categories

In the section 3, we presented the following four categorizations of words:

1. Convergence to a constant (S-curve) ($Y < 0$, $\alpha > 0$).
2. Finite-time divergence (Deadline effects) ($Y > 0$, $\alpha > 0$)
3. Divergence after infinite time (Asymptotic power-law function) ($Y > 0$, $\alpha < 0$)
4. Finite-time divergence of first-order derivatives ($Y < 0$, $\alpha < 0$)

In this section we give examples of words in each of those four categories for blog data. Specifically, (i) $\alpha > 0$ and $Y < 0$ are shown in table A2, (ii) $\alpha > 0$ and $Y > 0$ in table A3, (iii) $\alpha < 0$ and $Y > 0$ in table A4, and (iv) $\alpha < 0$ and $Y < 0$ in table A5.

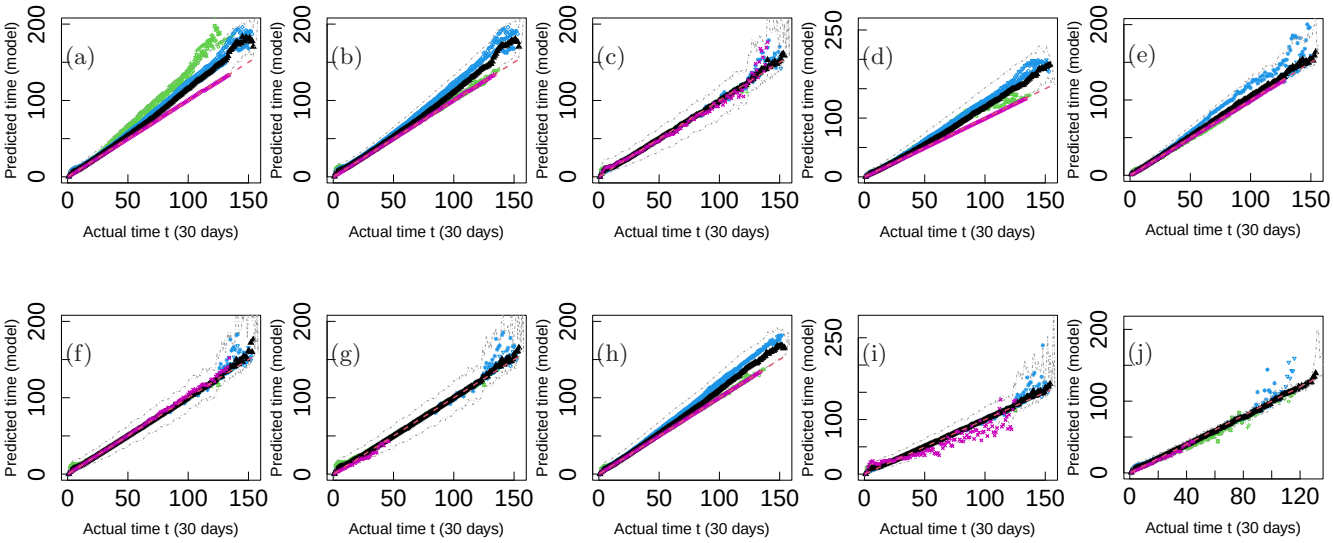


FIG. A3: Comparison of the descriptiveness of the dynamics of word count time series in various models using the time description (Inverse functions of solution of differential equation, $t = F^{(-1)}(y|\alpha, Y)$). If the model explains the data well, the graph will be close to the $y = x$ line shown by the red dashed line. The y-axis corresponds to the left-hand side $F^{(-1)}(y_j(t)|\alpha_j, Y_j)$ and the x-axis to the right-hand side t, where the differential equation is written as $\frac{dy(t)}{dt} = f(y|\alpha, Y)$ and the its solution as $y(t) = F(t|\alpha, Y)$ and its inverse function as $t = F^{(-1)}(y|\alpha, Y)$. Specifically, we plot the median quantity with respect to words given by Eq. A6 using Eq. A14 (See also the subsection A7.5). The ensemble median over all data is plotted in black triangles and also the ensemble median grouped by proposed model's (Eq. A1) parameters $\alpha_j^{(0)}$ and $Y_j^{(0)}$ is plotted. In case of $Y_j^{(0)} > 0$, we plott in green circles for $\alpha_j^{(0)} = 0.5$, green pluses for $\alpha_j^{(0)} = 1.0$, for green triangles up and down $\alpha_j^{(0)} = 1.5$, blue diamonds for $\alpha_j^{(0)} = -0.5$, blue triangles point down for $\alpha_j^{(0)} = -1.0$ and in the case of $Y_j^{(0)} < 0$ magenta crosses. (a) Logistic equation given by Eq. A1, (b) Y-sign extended logistic equation given by Eq. A2, (c) Single factor power-law model given by Eq. A3, (d) (Y-sign extended) Bass model given by Eq. A7, (e) Constant model given by Eq. A8, (f) First factor power-law model given by Eq. A9, (g) Second factor power-law model (Proposed model) given by Eq. A10, (h) Inside power-law model given by Eq. A11, (i) Y-sign positive-restricted second factor power-law model given by Eq. A12 and (j) Y-sign negative-restricted second factor power-law model given by Eq. A13.

Model	Prediction error R	Training Error S
(a) Logistic	0.64 [0.63,0.65]	0.73 [0.73,0.74]
(b) Y-sign extended Logistic	0.69 [0.68,0.70]	0.65 [0.64,0.66]
(c) Single power-law	0.45 [0.44,0.46]	0.63 [0.63,0.64]
(d) Y-sign extended Bass model	0.75 [0.74,0.76]	0.73[0.72-0.74]
Bass model ($Y < 0$)	0.67 [0.66,0.68]	0.72 [0.71,0.73]
(e) Constant factor	0.65 [0.64,0.66]	0.53 [0.52,0.54]
(f) First power-law	0.61 [0.60,0.62]	0.49 [0.48,0.50]
(g) Second power-law (Proposed model)	-	-
(h) Inside power-law	0.63[0.62,0.64]	0.39 [0.38,0.40]
(i) Positive model	0.46 [0.45,0.47]	0.54 [0.53-0.55]
(j) Negative model	0.64 [0.63,0.65]	0.69 [0.68-0.70]
SARIMA	0.52 [0.51,0.53]	0.61 [0.60-0.62]
Prophet	0.59 [0.58,0.60]	0.34 [0.33-0.34]

95% confidence intervals in brackets.

TABLE A1: Winning ratio of prediction and training errors of the proposed model compared to other models

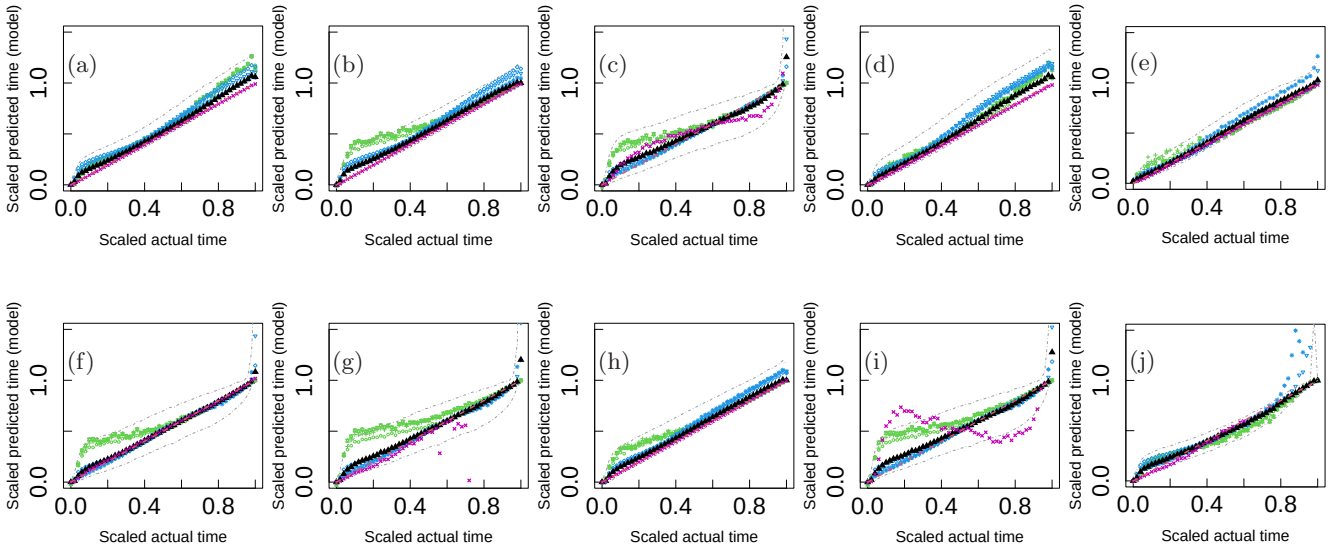


FIG. A4: Comparison of the descriptiveness of the dynamics of word count time series in various models using the scaled inverse functions of solution of differential equation, $F^{(-1)}(t|\alpha_j, Y_j)/T_j$. This figure is corresponding figure of Fig. A3 for the time scale normalised to 1 for the entire growth period (see Eq. A17). (a) Logistic equation given by Eq. A1, (b) Y-sign extended logistic equation given by Eq. A2, (c) Single factor power-law model given by Eq. A3, (d) (Y-sign extended) Bass model given by Eq. A7, (e) Constant model given by Eq. A8, (f) First factor power-law model given by Eq. A9, (g) Second factor power-law model (Proposed model) given by Eq. A10, (h) Inside power-law model given by Eq. A11, (i) Y-sign positive-restricted second factor power-law model given by Eq. A12 and (j) Y-sign negative-restricted second factor power-law model given by Eq. A13.

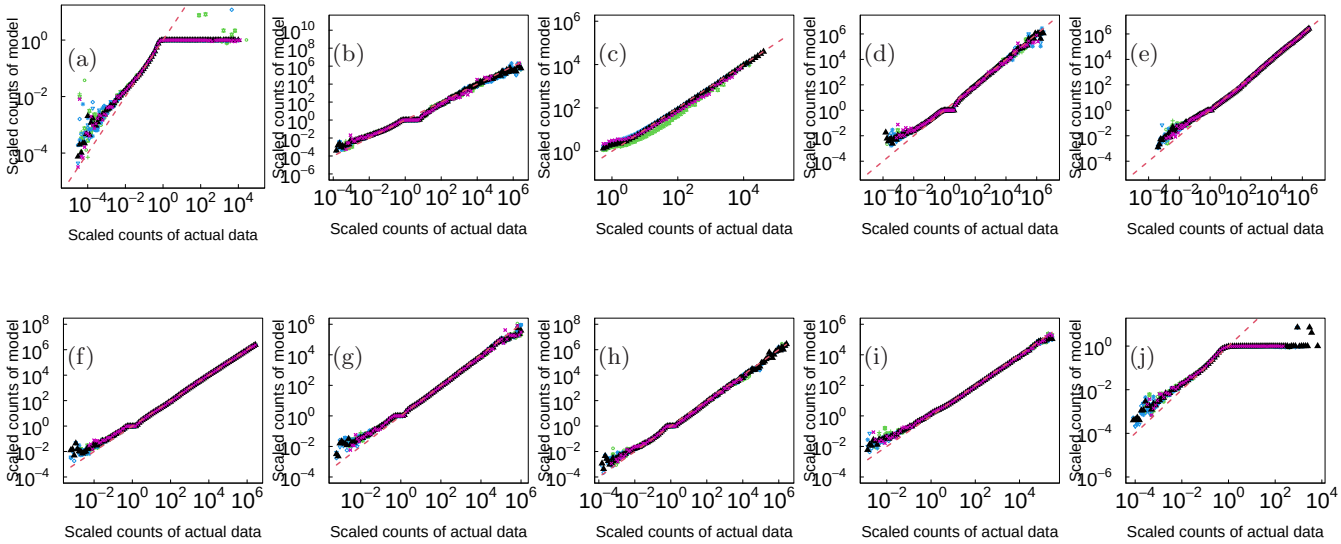


FIG. A5: Comparison of the descriptiveness of the dynamics of word count time series in various models using the solution of (scaled) differential equation $F(t|\alpha_j, Y_j)/|Y_j|$. If the model explains the data well, the graph will be close to the $y = x$ line shown by the red dashed line. The y-axis corresponds to the left-hand side of $F(t|\alpha_j, Y_j)/|Y_j|$ (Theoretical value from t) and the x-axis to the right-hand side of $y_j(t)/|Y_j|$ (observed value), where the differential equation is written as $\frac{dy(t)}{dt} = f(y(t)|\alpha_j, Y_j)$ and the its solution as $y = F(t|\alpha_j, Y_j)$. Specifically, we plot the median quantity with respect to words given by Eq. A6 using Eq. A18, which is scaled by the model's scale parameter Y. The ensemble median over all data is plotted in black triangles, and also the ensemble median grouped by the proposed model's (Eq. A1) parameters $\alpha_j^{(0)}$ and $Y_j^{(0)}$ is plotted. In case of $Y_j^{(0)} > 0$, we plot in green circles for $\alpha_j^{(0)} = 0.5$, green pluses for $\alpha_j^{(0)} = 1.0$, for green triangles up and down $\alpha_j^{(0)} = 1.5$, blue diamonds for $\alpha_j^{(0)} = -0.5$, blue triangles pointing down for $\alpha_j^{(0)} = -1.0$ and in the case of $Y_j^{(0)} < 0$ magenta crosses. (a) Logistic equation given by Eq. A1, (b) Y-sign extended logistic equation given by Eq. A2, (c) Single factor power-law model given by Eq. A3, (d)(Y-sign extended) Bass model given by Eq. A7, (e) Constant model given by Eq. A8, (f) First factor power-law model given by Eq. A9, (g) Second factor power-law model (Proposed model) given by Eq. A10, (h)Inside power-law model given by Eq. A11, (i)Y-sign positive-restricted second factor power-law model given by Eq. A12 and (j)Y-sign negative-restricted second factor power-law model given by Eq. A13.

Word	English Translation	Romanization	Note
タブレット端末	Tablet terminal	TaburretoTanmatsu	Information equipment
リツイート	Retweet	RiTsuiito	SNS term
HKT48	HKT48	HKT48	Japanese idol girl group
スカイツリー	Sky Tree	SukaiTsurii	Architectural monument
LINEスタンプ	LINE stamp	LINEsutanpu	LINE is the most used mobile messenger application in Japan
東京スカイツリー	Tokyo Sky Tree	ToukyouSukaiTsurii	Architectural monument
イクメン	Ikumen	Ikumen	Catchphrase: men raising children
黒子のバスケ	Kuroko's basketball	KurokonoBasuke	Cartoon title
アンジュルム	Anjurum	Anjyurumu	Dance group
ウェアラブル端末	Wearable device	UearaburuTanmatsu	Technology term
国家戦略特区	National Strategic Special Zone	KokkaSenryakuTokku	Areas with special legal treatment
USTREAM	USTREAM	USTREAM	Video distribution service
小島瑠璃子	Ruriko Kojima	KojimaRuriko	Name of TV Personality
坂口杏里	Anri Sakaguchi	SakaguchiAnri	Name of TV Personality
ウサイン・ボルト	Usain Bolt	UsainBoruto	Track and field player
アスキー・メディアワークス	ASCII Media Works	AsukiiMediaWaakusu	Publisher name
神ってる	Be godly	Kamitteru	Baseball buzzword
株式会社KADOKAWA	KADOKAWA Co., Ltd.	KabushikiGaishiya KADOKAWA	Media company name
日笠陽子	Yoko Hikasa	HikasaYouko	Voice actor name
オワコン	Owakon	Owakon	Slang for out of fashion
人工多能性幹細胞	Artificial pluripotent stem cells	JinkouTanouseiKanSaibou	Biological term
カイロ・レン	Cairo Len	KairoRen	Person name in the movie
シシド・カフカ	Shishid Kafka	ShishidoKafuka	Actress name
サッスオーロ	Sassuolo	Sassuoro	Name of soccer team
肉食系女子	Carnivorous girls	NikuShyokuKeiJyoshi	Buzzwords for a woman who is active in romance
水卜麻美	Asami Miura	MiuraAsami	The one of most famous female announcer name in Japan
Astell&Kern	Astell & Kern	Astell & Kern	Audio maker name
井浦新	Arata Iura	IuraArata	Actor name
美人時計	Beautiful woman clock	BijinDokei	Website that displays a beautiful woman every hour
南野拓実	Takumi Minamino	MinaminoTakumi	Soccer player
八戸学院光星	Hachinohe Gakuin Kousei	HachinoheGakuinKousei	High school famous for a baseball
クリス・ヘムズワース	Chris Hemsworth	KurisuHemuzuwaasu	Actor name
ソン・ジュンギ	Song Junggi	SonJyungi	Actor name
ウェアラブルカメラ	Wearable camera	UearaburuKamera	Technology term
稲嶺進	Susumu Inamine	InemineSusumu	Governor of okinawa prefecture name
標的型メール	Target email	HyoutekiGataMeiru	Malicious Targeted Email
スカパーJSAT	SKY PerfecTV JSAT	SukapaaJSAT	Satellite TV company name
大塚角満	Kadoman Otsuka	OotsukakaKadoman	Game writer name
ミライース	Daihatsu Mira e:S	Miraiisu	Car name
ヤンマースタジアム長居	Yanmar Stadium Nagai	YanmaaSutajiamuNagai	Soccer stadium name
涙活	Tear-jerking activities	RuiKatsu	Activities to relieve stress through conscious crying

TABLE A2: Example of words for $\alpha > 0$ and $Y < 0$ (Convergence to a constant or S-curve) for blog data. Specifically, the top 40 words in frequency that satisfy the following conditions: (i) a growth period of at least 48 timestamps (about 4 years) (ii) $\alpha > 0.1$ (iii) $Y < 0$.

Word	English Translation	Romanization	Note
ビットコイン	Bitcoin	BittoKoin	Cryptocurrency name
リオ五輪	Rio Olympics	RioGorin	Sport event
リオデジャネイロ五輪	Rio de Janeiro Olympics	Riodejyaneirogorin	Sport event
ソチ五輪	Sochi Olympics	SochiGorin	Sport event
清武弘嗣	Hiroshi Kiyotake	KiyotakeHiroshi	Soccer player name
ピコ太郎	Pico Taro	PikoTarou	Comedian whose videos attracted worldwide attention
iPhone7	iPhone7	iPhone7	Smartphone model
森脇稔	Minoru Moriwaki	MoriwaKiminoru	Baseball director name
EU離脱	Withdrawal from the EU	EURidatsu	Political terms
IFTTT	IFTTT	IFTTT	Web service name
シャドバ	Shadowverse	Shyadoba	Game name
ソードアート・オンライン	Sword Art Online	SoodoAatoOnrain	Game name
コウノドリ	Kounodori: Dr. Stork	Kounodori	TV drama name
山本美月	Mizuki Yamamoto	YamamotoMizuki	Young actoress name
川内原発	Kawauchi nuclear power plant	KawauchiGenpatsu	Nuclear power plant name
S660	S660	S660	Car name
マクロン	Macron	Makuron	President French name
ユニットコム	Unitcom	Yunnitokomu	PC shop name
カズレーザー	Kaz laser	Kazureezaa	Comedian name
オバマケア	Obamcare	ObamaKea	Political terms
シェールガス	Shale gas	SheiruGasu	Economic term
広州恒大	Guangzhou Kenzu	KoushyuuKoudai	Soccer team name
Jアラート	J alert	JAraato	Japan emergency alert system
Cortana	Cortana	Cortana	Digital assistant system name
リオデジャネイロオリンピック	Rio de Janeiro Olympics	RiodejyaneiroOrinppiku	Sport event
貴ノ岩	Takanoiwa	Takanoiwa	Sumo player name
ソチオリンピック	Sochi Olympics	SochiOrinppiku	Sport event
南シナ海問題	South China Sea problem	Minamishinakaimondai	Political terms
オクタコア	Octa-core processor	OkutaKoa	Computer parts
海街diary	Sea Town DIARY	UmigaiDaiarii	Movie name
社会保障と税の一体改革	Integrated reform of social security and tax	ShyakaiHoshiyouTo ZeinoIittaiKaikaku	Political term
山田哲人	Tetsuto Yamada	YamadaTetsuto	Baseball player name
清宮幸太郎	Kotaro Kiyomiya	SeimiyaKoutarou	Baseball player name
ジュラシック・ワールド	Jurassic World	JyurasshikuWaarudo	Movie name
マイナス金利政策	Negative interest rate policy	MainasuKinriSeisaku	Economic term
永野芽郁	Meiku Nagano	NaganoMeiku	Young actoress name
日本エレキテル連合	Japan Electric Generator Union	NipponErekiteruRengou	Comedian who won a buzzword award
KCON	KCON	KCON	Events on Korean popular culture
噴火警戒レベル	Eruption alert level	FunkaKeikaiReberu	Disaster term
グノシー	Gnossy	Gunoshii	Information curation services on smartphones

TABLE A3: Example of words for $\alpha > 0$ and $Y > 0$ (Finite-time divergence or Deadline effects) for blog data. Specifically, the top 40 words in frequency that satisfy the following conditions: (i) a growth period of at least 48 timestamps (about 4 years) (ii) $\alpha > 0.1$ (iii) $Y > 0$.

Word	English Translation	Romanization	Note
スマホ	Smartphone	Sumaho	Smartphone
モデルプレス	Model press	ModeruPuresu	Net news site
インスタグラム	Instagram	Insutaguramu	SNS term
Xperia	Xperia	Xperia	Smartphone model
妊活	Pregnancy preparation activity	Ninkatsu	Buzz word
SKE48	SKE48	SKE48	Japanese idol girl group
タブレット端末	Tablet terminal	TaburretoTanmatsu	Information equipment
bit.ly	bit.ly	bit.ly	Short URL service
ニコニコ生放送	Nico Nico Live Broadcast	NikonikoNamaHousou	Internet live broadcasting Service
ビッグデータ	Big data	Biggudeeta	Information technical term
公式Twitter	Twitter verification mark	KoushikiTwitter	SNS term
メルカリ	Mercari	Merukari	Online flea market application
クラウドファンディング	Crowdfunding	KuraudoFuandingu	Economic term
習近平	Xi Jinping	ShyuuKinpei	Chinese leader
goo.gl	goo.gl	goo.gl	Short URL service
熊本地震	Kumamoto earthquake	KumamotoJishin	Earthquake name
ももクロ	Momokuro	Momokuro	Japanese idol girl group
ふるさと納税	Hometown tax payment	FurusatoNouzei	Tax deduction system
TechinsightJapan	TechinsightJapan	TechinsightJapan	Net news site
ニコ生	Nico Nico Live Broadcast	Nikonama	Internet live broadcasting Service
スマートフォンアプリ	Smartphone app	SumaatofonApuri	Smartphone term
ガラケー	Flip phone	Garakee	Feature phone before smartphone
日馬富士	Hima Fuji	KusamaFujisaki	Sumo wrestler name
朝日新聞デジタル	Asahi Shimbun Digital	AsahiShinbunDejitaru	News site
Androidアプリ	Android app	Androidapuri	Smartphone term
nanapi	nanapi	nanapi	Online know-how sharing service
指原莉乃	Rino Sashihara	SasuharaRino	Young singer and actoress name
スマホアプリ	Smartphone app	SumahonApuri	Smartphone term
格安スマホ	Low-Cost smartphone	KakuyasuSumaho	Smartphone term
みんなの党	Everyone's party	MinnanoTou	Political party name
松山英樹	Hideki Matsuyama	MatsuyamaHideki	Golf player name
スマートウォッチ	Smart watch	SumaatoUochi	Smartphone term
pixiv	pixiv	pixiv	Online community service for artists
格安SIM	Low-Cost Sim Card	KakuyasuSIM	Smartphone term
スマホゲーム	Smartphone game	SumahoGemu	Smartphone term
レコチョク	RecoChoku	Rekochiyoku	Music distribution site
SHINee	Shinee	SHINee	Korean idol boy group
AppStore	AppStore	AppStore	Smartphone term
Twitterアカウント	Twitter account	TwitterAkaunto	SNS term
広瀬すず	Hirose Suzu	HiroseSuzu	Young Actoress name

TABLE A4: Examples of words for $\alpha < 0$ and $Y > 0$ (Divergence after infinite time or Asymptotic power-law function) for blog data. Specifically, the top 40 words in frequency that satisfy the following conditions: (i) a growth period of at least 48 timestamps (about 4 years) (ii) $\alpha < -0.1$ (iii) $Y > 0$.

Word	English Translation	Romanization	Note
Android携帯	Android mobile	Androidkeitai	Smartphone term
CULEN	CULEN	CULEN	Entertainment office name
メッセニア	Messenia	Messenia	Place name

TABLE A5: Example of words for $\alpha < 0$ and $Y < 0$ (Finite-time divergence of first-order derivatives) for blog data. Specifically, these are words that satisfy the following conditions: (i) a growth period greater than 48 timestamps (about 4 years) (ii) $\alpha > 0.1$ (iii) $Y < 0$. Words in this category have a large discrepancy between the theoretical line and the real data, i.e., the model does not work well.